الجمهورية الجزائرية الديمقراطية الشعبية
People's Democratic Republic of Algeria
وزارة التعليم العالي والبحث العلمي
Ministry of Higher Education and Scientific Research
جامعة غرداية
University of Ghardaia
كلية العلوم والتكنولوجيا
Faculty of Science and Technology
قسم الآلية والكهروميكانيك
Department of Automatics and Electromechanics

Registration number
...../...../.....

END OF STUDIES' DISSERTATION

Submitted in Partial Fulfillment of the Requirements for the Master's Degree

Domain: Science and Technology
Field: Automatic
Speciality: Automatic and Systems

Theme

Modeling and control methods of dynamic wireless power transfer (WPT) system

Presented by:
Bettache tarek
Rehaiem Kaouther

Publicly supported on: 17/09/2024
Jury Members

BOUKHARI Hamed	MCB	Univ. Ghardaïa	**President**
BECHOUAT Mohcen	PROF	Univ. Ghardaïa	**Examiner**
FIHAKHIR Amine	MCB	Univ. Ghardaïa	**Examiner**
BEKKAR Belgacem	MCA	Univ. Ghardaïa	**Supervisor**

Academic year: 2023/2024

Abstract

Dynamic wireless power transfer (WPT) technology with broad prospects provides a safe and convenient solution for electric vehicle charging and promotes the development of electric vehicle industry. This note introduces the wireless power transfer and time-dependent development and battery charging optimization method by DC-DC boost converter using perturbation and observation (P&O) using MEPT algorithms. The control strategies and design of this controller are proposed based on the analysis of WPT circuit and power converter model. The effectiveness of the simulation method is verified.

Keywords : Boost converter, MEPT, perturbation and observation (P&O , Simulation WPT

Résumé

La technologie de transfert dynamique de puissance sans fil (WPT), qui offre de vastes perspectives, constitue une solution sûre et pratique pour la recharge des véhicules électriques et favorise le développement de l'industrie des véhicules électriques. Cette note présente la méthode d'optimisation du transfert de puissance sans fil, du développement en fonction du temps et de la charge de la batterie par convertisseur DC-DC boost à l'aide de la perturbation et de l'observation (P&O) en utilisant les algorithmes MEPT. Les stratégies de contrôle et la conception de ce contrôleur sont proposées sur la base de l'analyse du circuit WPT et du modèle de convertisseur de puissance. L'efficacité de la méthode de simulation est vérifiée.

Mots-clés: Convertisseur de puissance, MEPT, perturbation et observation (P&O), Simulation WPT

ملخص

تقنية نقل الطاقة اللاسلكية الديناميكية (WPT) توفر حلاً آمناً ومريحاً لشحن المركبات الكهربائية، مما يعزز تطور صناعة السيارات الكهربائية بفضل آفاقها الواسعة. تقدم هذه المذكرة مقدمة حول تقنية نقل الطاقة اللاسلكية وتطورها بمرور الوقت، بالإضافة إلى تحسين عملية شحن البطاريات باستخدام محول رفع التيار المستمر (DC-DC Boost Converter) عبر تقنية "الاضطراب والمراقبة" (P&O) باستخدام خوارزميات MEPT. تم اقتراح استراتيجيات التحكم وتصميم هذا المتحكم بناءً على تحليل دائرة WPT ونموذج محول الطاقة. وقد تم التحقق من فعالية طريقة المحاكاة المستخدمة.

الكلمات المفتاحية: محول رفع التيار، MEPT، الاضطراب والمراقبة (P&O)، المحاكاة، نقل الطاقة اللاسلكية

Contents

List of Figures

List of Abbreviations

WPT: Wireless Power Transfer

MPPT: Maximum power Point Tracking

P&O: Perturbation and Observation

EVs: Electric Vehicles

PMA: Power Matters Alliance

AC: alternating current

DC: direct current

EMF: electromotive force

IPT: Inductive Power Transfer

ESR: equivalent series resistance

ESL: equivalent series inductance

EMI: electromagnetic interference

FOD: Foreign Object Detection

AWP: Alliance for Wireless Power

DWPT: Dynamic Wireless Power Transfer

DWC: Dynamic Wireless Charging

PHEV: plug-in hybrid electric vehicle

BMS: battery management system

SPS: solar power satellites

PDM: pulse-density modulation

PWM: pulse-width modulation

MEPT: Maximum Efficiency Point Tracking

General introduction

Wireless Power Transfer (WPT) technology has emerged as a transformative solution for transmitting electrical energy without the need for physical connectors, leveraging electromagnetic fields to transfer power across an air gap. WPT has found extensive applications across various fields, including consumer electronics, electric vehicles (EVs), and medical devices. This technology, while promising, requires careful consideration of efficiency, system architecture, and optimization strategies, especially when applied to dynamic systems such as electric vehicle charging [1] [2].

The focus of this dissertation is on the modeling and control methods of a dynamic wireless power transfer (WPT) system. Dynamic WPT, a critical innovation in electric vehicle charging, allows vehicles to be charged while in motion, offering significant convenience and efficiency. This research narrows its focus to optimizing the control strategies for dynamic WPT, particularly by employing a boost converter with Maximum power Point Tracking (MPPT) algorithms like Perturbation and Observation (P&O) [3]. The scope of the research includes developing a robust simulation model that verifies the system's effectiveness in real-world applications.

The relevance of this study lies in the growing demand for efficient wireless charging systems, especially for electric vehicles, where seamless charging solutions are essential to overcoming the limitations of traditional plug-in methods. Current literature emphasizes various WPT technologies, but further research is needed to enhance the efficiency and control strategies in dynamic applications. By building on previous advancements in WPT and exploring new control methods, this research aims to contribute to the development of more efficient and scalable wireless charging systems.

The primary research question driving this dissertation is: How can dynamic WPT systems be optimized to maximize efficiency, particularly in electric vehicle applications? The objectives include designing a control system for dynamic WPT, simulating its performance, and evaluating its efficiency.

The structure of this dissertation is as follows:

- **Chapter 1** provides a detailed literature review, examining the historical development, technical breakthroughs, and current applications of WPT systems.
- **Chapter 2** focuses on the design and modeling of WPT systems, with a particular emphasis on the control strategies for boost converters in dynamic wireless charging.

- **Chapter 3** presents the simulation results and discusses the performance of the proposed system, evaluating its efficiency under different conditions. The dissertation concludes with a summary of findings and recommendations for future research.

Chaptre 1: General aspects

1.1 Introduction

More than a century ago, the idea of transmitting electricity via radio waves without a physical connection between the source and the receiver was first proposed. Research in wireless energy transfer wires has produced ground-breaking results in numerous fields of expertise, such as consumer electronics, automotive, and industrial control process [1-3]. WPT has been employed in different industries, including consumer electronics (phones, computers, audio players, tablets, etc. Medical applications, wireless power delivery removes the need for transdermal or percutaneous wires, which can be cumbersome and prone to infection.

1.1.1 Definition WPT

Wireless Power Transfer (WPT) is the transmission of electrical energy without the need for

physical connectors or wires. This technology leverages electromagnetic fields to transfer power from a source to a load across an air gap [2]. Wireless power transmission is used in areas, the most important of which are: Consumer Electronics (Wireless charging for devices like smartphones, tablets...), Electric Vehicles (EVs), Medical Devices, Aerospace and Defense (Operating drones and remote sensing equipment), Smart Homes and IoT: Integrating wireless power into home automation systems.

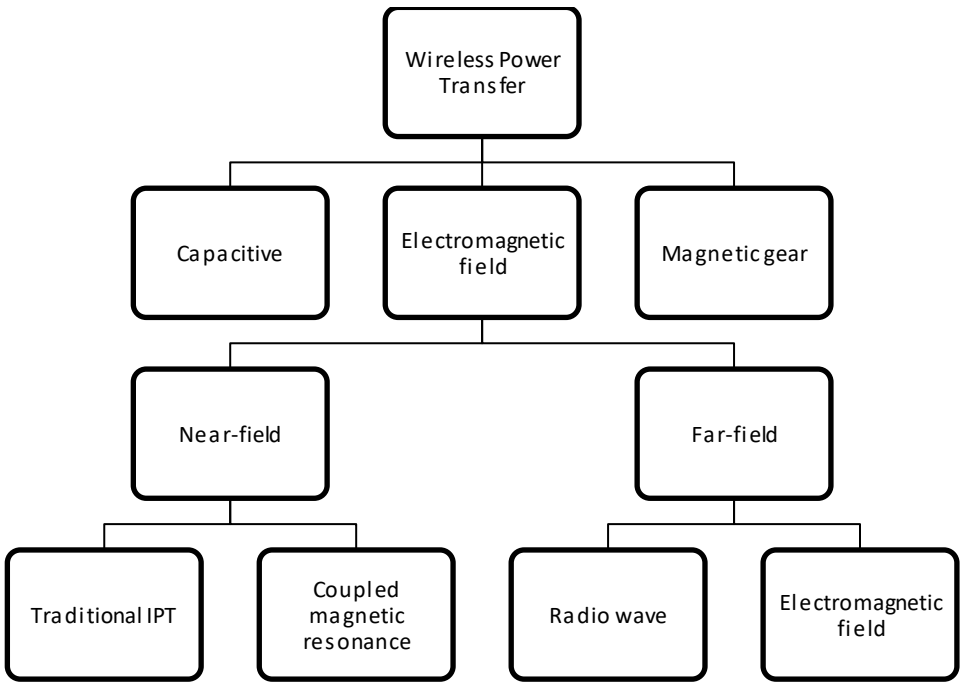

Figure 1-1: Classification of WPT technologies [1].

1.2 Historical Background and Evolution of WPT

1.2.1 Theoretical Foundation

The theoretical foundation of Wireless Power Transfer (WPT) is rooted in the early 19th century with Hans Christian Oersted's discovery that electric current generates a magnetic field. This discovery led to the formulation of fundamental laws by André-Marie Ampère, Jean-Baptiste Biot, and Félix Savart, which describe the behavior of magnetic fields. The unification of electricity and magnetism was achieved through James Clerk Maxwell's equations in 1864, culminating in his influential 1873 publication "A Treatise on Electricity and Magnetism." These contributions established the modern understanding of electromagnetism, setting the stage for advancements in wireless power transfer [2].

1.2.2 Technical Breakthroughs and Research Projects

The evolution of WPT has been marked by significant technical breakthroughs. In 1888, Heinrich Hertz experimentally confirmed the existence of electromagnetic waves, a pivotal moment for wireless communication. Nikola Tesla, a pioneer in electrical engineering, conducted groundbreaking experiments on long-distance wireless power transmission using microwave technology. In 1896, Tesla successfully transmitted microwave signals over a distance of 48 kilometers. In 1899, he achieved another major milestone by transmitting high-frequency electric power over 25 miles to light 200 bulbs and power an electric motor. Despite these successes, Tesla's methods were shelved due to safety concerns related to high voltage emissions.

Tesla also made notable contributions to magnetic field technology with the invention of the Tesla coil and the construction of the Wardenclyffe Tower in 1901 for wireless energy transmission through the ionosphere. However, due to technological limitations, these ideas were not widely developed or commercialized at the time. During the 1920s and 1930s, the invention of magnetrons enabled the conversion of electricity into microwaves, facilitating wireless power transfer over long distances. However, the lack of methods to convert microwaves back into electricity led to a temporary halt in the development of wireless charging.

The practical realization of microwave power transfer came in 1964 with W. C. Brown's invention of the rectenna, which efficiently converted microwaves to electricity. Brown demonstrated this technology by powering a model helicopter (Figure 1-2-c), inspiring further research into microwave-powered systems, including solar power satellites (SPS) by NASA. In 1975, Brown achieved a significant milestone by beaming 30kW over a distance of 1 mile with 84% efficiency at the Venus Site of JPL's Goldstone Facility (Figure 1-2-d). These advancements spurred further development in large-scale microwave transfer technologies.

1.2.3 Commercialization

The commercialization of WPT gained momentum in the 1990s with the rise of portable electronic devices. Early commercial products explored both far-field and near-field wireless charging techniques. In 2007, the introduction of Witricity technology demonstrated the practicality and efficiency of mid-range non-radiative wireless charging (Figure 1-2-e). Various radiative wireless

charging systems, such as the Cota system, PRIMOVE, and Powercast's wireless rechargeable sensor system (Figure 1-2-f), were also commercialized during this period.

In recent years, consortiums such as the Wireless Power Consortium (WPC), Power Matters Alliance (PMA), and the Alliance for Wireless Power (AWP) have developed international standards for wireless charging. These standards have been widely adopted in consumer electronics, such as smartphones and wireless chargers (Figure 1-2-g). A notable recent development is the magnetic MIMO technology, which utilizes multi-antenna beamforming based on magnetic waves (Figure 1-2-h). This technology represents a significant advancement in the field of WPT, highlighting the ongoing evolution and commercialization of wireless power transfer technologies [4] [1].

These historical developments reflect the continuous progress and increasing interest in integrating wireless charging into everyday devices and applications, driven by advancements in technology and the growing demand for convenient and efficient power transfer solutions [5].

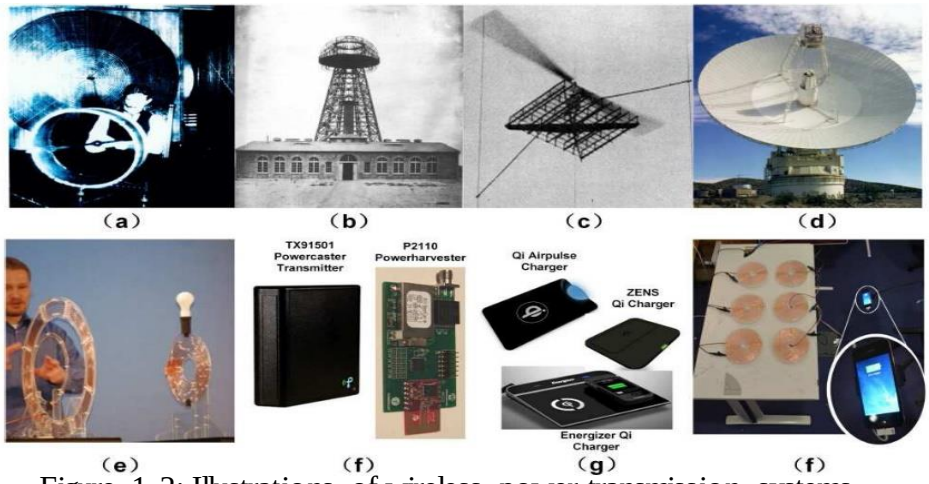

Figure 1-2: Illustrations of wireless power transmission systems.

1.2.4 Significance of WPT in Modern Applications

WPT has several significant applications in modern technology [1]

1) **Consumer Electronics:** WPT enables the wireless charging of smartphones, tablets, wearable, and other portable devices. This eliminates the need for cables and connectors, providing convenience to users.
2) **Electric Vehicles (EVs):** WPT can be used to charge electric vehicles wirelessly, offering a convenient and efficient way to charge vehicles without the need for physical connections. This technology is particularly useful for charging EVs in public places and at home.
3) **Medical Devices:** WPT is used in various medical devices such as implantable devices (e.g., pacemakers, neurostimulators) to power them wirelessly, eliminating the need for frequent battery replacements or wired connections.

4) **Industrial Applications:** WPT can be used in industrial applications to power sensors, actuators, and other devices in hard-to-reach without the need for maintenance of physical connections.
5) **Infrastructure and IoT:** WPT can be integrated into infrastructure and IoT devices to provide power without the need for frequent battery replacements or complex wiring.
6) **Military and Aerospace:** WPT can be used in military and aerospace applications to power sensors, communication devices, and other equipment without the need for physical connections, reducing the risk of damage and improving reliability.

Overall, WPT offers a versatile and convenient way to provide power to various devices and systems in modern applications, improving efficiency, convenience, and reliability.

1.3 Principle and fundamentals of Magnetic Field Coupling

When electrical energy from an alternating current (**AC**) power supply such as a commercial power supply or from a direct current (**DC**) power supply such as solar cells is converted to high-frequency electrical energy by using a high-frequency inverter, the wireless feeding device (Tx) releases electrical energy through a transmission device into space. Then, the receiving system (Rx) converts the electrical power into DC in the recipient electrical appliance. A key feature of noncontact electricity transmission is the distribution of electromagnetic energy over space by using an electromagnetic field or wave.

Such transmission requires an electricity conversion apparatus such as a high-frequency inverter. Therefore, improvement in the efficiency of the electrical power transmission of the se converters is also important. Since electromagnetic energy is distributed over space, considering the medical and environmental influence of electromagnetic waves is important [6].

1.3.1 Concept of the coupler

A device to transduce power between circuit and air is the most important component in the WPT system. To integrate power electronics-based and RF-based WPT technologies, a problem is that there is no terminology of this device. For example, the term **coil** describes the shape of the device, which cannot be applicable for electric field coupling-type WPT that uses an electrode. Furthermore, there are two meanings of the term coil. One acts as an inductor, which is used in kHz band WPT system. The other acts as a self-resonant resonator, which can be seen mainly in MHz band WPT system. Both ends are opened. In the circuit, this coil can be described as inductor and capacitor (LC) resonator, not inductor. The term **resonator** is also often confusing. In the kHz band WPT system, coupling coil and resonant capacitor consist of a **resonator**. However, sometimes resonator designates only the coupling coil [4].

The term **antenna** is not adequate for all WPT systems because coupled resonant WPT is used in the near-field region, not radiating the far-field region. In this section, the term **coupler** is defined as a device that transduces electric power between circuit and air. In this definition, coupling coil, antenna, and electrode are involved in coupler. For a resonator with a coupling coil and a resonant

capacitor, only the coupling coil is a coupler. Coupler may be a self-resonant device or a non-resonant device [4].

1.3.1.1 Unified model based on resonance and coupling

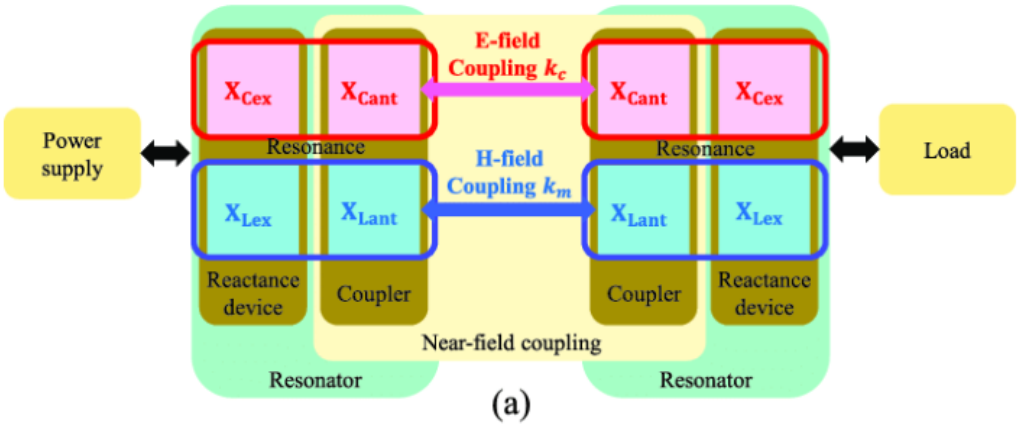

Figure 1-3: Unified model for coupled-resonant WPT

Unified model of the coupled-resonant WPT is shown in Figure 1-3This model enables us to explain coupled-resonant WPT from the viewpoint of resonance and coupling which is uniformly applicable for power electronics-based WPT and RF-based WPT [4].

Power supply is connected to the transmitting (Tx) resonator. Load is connected to the receiving (Rx) resonator. The resonator consists of a coupler and a reactance element. A reactance element is a device that has reactive impedance, but not intended to interact between air and circuit. For example, coupling coil is a coupler, but coil in matching circuit is a reactance element. The coupler has capacitive and inductive reactance X_{Ccp} and X_{Lcp}, respectively. The reactance element has capacitive and inductive reactance X_{Cex} and X_{Lex}, respectively [4].

The phenomena **resonance** is explained as follows. The inductive reactance of the resonator consists of X_{Lex} and X_{Lcp}. The capacitive reactance of the resonator consists of X_{cex} and X_{Ccp}. The resonance occurs at the frequency in which the inductive and the capacitive reactance become same. Definition of resonant is an amount of the magnetic stored energy, and the electric stored energy becomes same in the resonator. The reactance device holds stored energy in a closed space, whereas the coupler holds it in an opened space [4].

The phenomena **coupling** is explained as follows. The capacitive reactance of the Tx resonator and the Rx resonator couple by electric field with a E-field coupling coefficient kc. The inductive reactance of the Tx resonator and the Rx resonator couple by magnetic field with a H-field coupling coefficient km [4].

By using this model, coupled-resonant WPT can be understood from the phenomena **coupling** and **resonant** separated out. as shown in Figure 1-3

1.3.2 Inductive Coupling in WPT Systems

The electromagnetic induction method is the method dipping up magnetic field energy by using a coil. Figure 1-4 assumes transformer coupling. In this manner, inherently larger coils will be used if it becomes larger electricity transmission.

Accordingly, the transmission distance increases in accordance with increasing power transmission. Furthermore, the area shown in

Figure 1-4 is obtained.

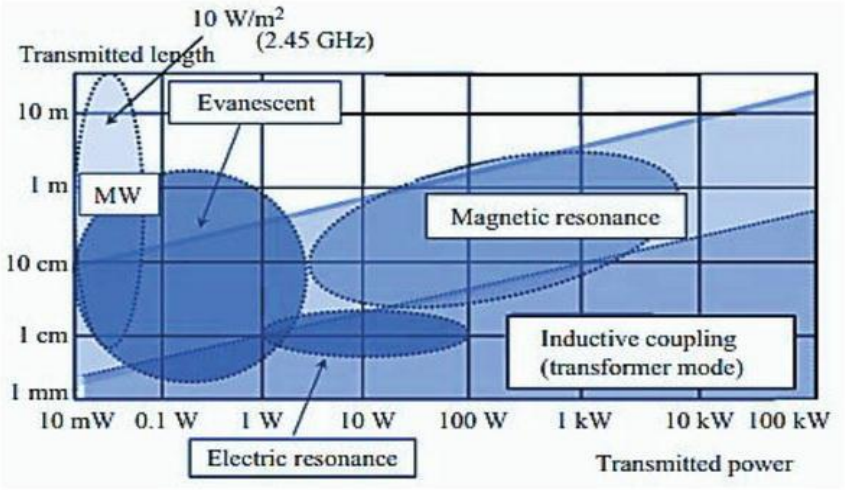

Figure 1-4: Proposed non-contact primary WPT methods [4].

illustrates an equivalent circuit for an electrical power transformer having a magnetic core. In the power transformer, an alternating magnetic flux in a magnetic core, which is always kept at a fixed maximum value relative to the alternating magnetic flux by a CV source, conveys electrical energy to a second side winding. Then, the electrical energy is transmitted. The load connected to a secondary coil consumes the electrical energy. It is desirable to maintain the coupling factor at 100% [4].

The condenser connected to the primary side mainly serves to compensate for reactive power or a power factor drop by a load connected to the second side. In the power transformer variant of the electromagnetic induction method, the circuitry design, including the condenser, has been performed from the point of view called the coil axis gap compensation between the primary and second coils [4].

In this manner, the transformer variant of the noncontact electricity transmission method points at a method to work under the circuit condition termed the CV drive in a method classified in an electromagnetic induction method. Of course, we will present a method that operates under other conditions in a subsequent section [4].

As mentioned earlier, Figure 1.4 depicts an equivalent circuit generally used for the analysis of the power transformer for electricity. In Figure 1.4, X‘1 is the leakage reactance of the transmission side. This reactance represents the magnetic flux f2, which does not link with the power receiving circuit. Similarly, X‘2 is the leakage reactance of the power receiving side. R1 and R2 are the winding

resistances of the power transmission and receiving coils, respectively. Y0 is the exciting admittance, and g0 is the exciting conductance representing the iron loss of the core material. [4]

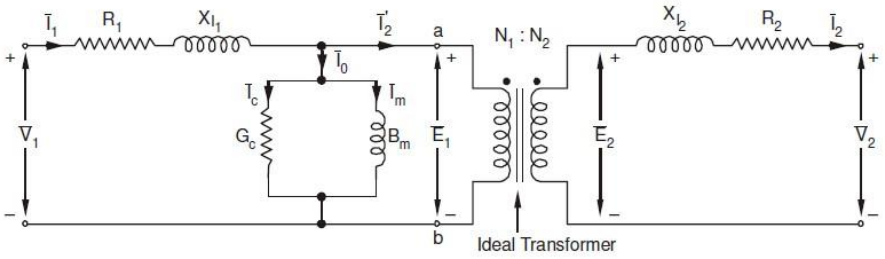

Figure 1-5: Equivalent Circuit of Transformer

1.4 Mechanism of WPT via Inductive Coupling

The mechanism of WPT via inductive coupling involves the following steps in Figure 1-6 [4]:

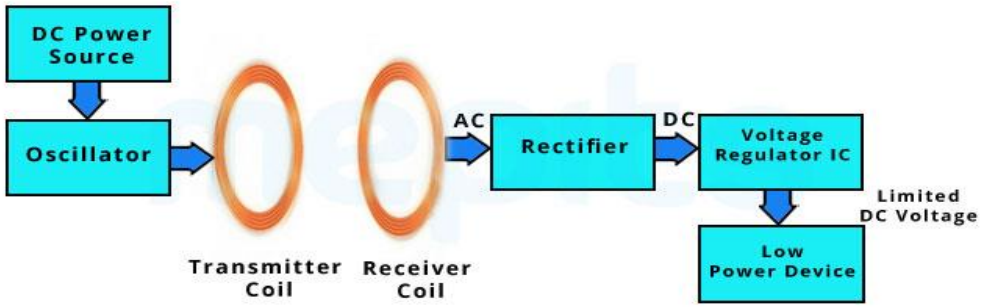

Figure 1-6: Mechanism Steps of WPT via Inductive Coupling

- **Generation of Alternating Current:** The transmitter generates an alternating current (AC) in the primary coil. This AC creates a changing magnetic field around the coil .
- **Induction of Current in the Receiver Coil:** The changing magnetic field induces an alternating current (AC) in the secondary coil of the receiver. This phenomenon is based on Faraday's law of electromagnetic induction, which states that a changing magnetic field induces an electromotive force (EMF) in a nearby conductor .
- **Rectification and Power Conversion:** The alternating current induced in the receiver coil is typically rectified to produce direct current (DC) using diodes. This DC can then be used to power various electrical devices or stored in batteries for later use. Additionally, power conversion circuits may be employed to match the voltage and current requirements of the load .
- **Efficiency Considerations:** Efficiency in WPT systems via inductive coupling is influenced by factors such as the distance between the transmitter and receiver coils, the

alignment between them, the properties of the coils (such as size, shape, and number of turns), and the frequency of the alternating current. Optimizing these parameters is crucial for maximizing the efficiency of power transfer.

- **Safety Considerations:** WPT systems must comply with safety regulations to ensure that they do not pose health risks to humans or interfere with other electronic devices. This includes limiting electromagnetic radiation and ensuring that the system operates within specified power limits.

1.4.1 Physical Representation of IPT in WPT Systems

Inductive Power Transfer (IPT) in WPT systems involves the transfer of electrical energy wirelessly through the use of electromagnetic fields. The physical representation of IPT in WPT systems primarily revolves around the design and arrangement of coils, along with other components. Here are the key aspects of the physical representation [7] [8]:

Coil Design:

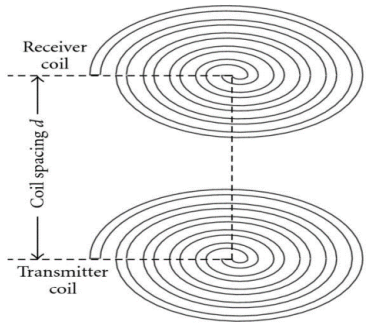

Figure 1-7 :Effect of variation of coil spacing between transmitter and receiver coils

Primary Coil (Transmitter Coil): This coil is responsible for generating an alternating magnetic field, which induces a current in the secondary coil.

Secondary Coil (Receiver Coil): Positioned within the range of the primary coil, the secondary coil receives the induced current, which is then used to power the device or charge a battery.

Coil Arrangement:

Coils are typically arranged in close proximity to each other to facilitate efficient power transfer. They may be aligned in a variety of configurations, such as parallel or perpendicular orientation, depending on the specific requirements of the application.

In some cases, multiple coils may be used on both the transmitter and receiver sides to improve power transfer efficiency, extend the operating range, or accommodate devices with different orientations.

Core Material:

Coils may be wound around a core material, such as ferrite or air, to enhance magnetic flux density and improve efficiency.

Ferrite cores are commonly used due to their high permeability, which helps to concentrate the magnetic field and reduce losses.

Resonant Circuits:

Resonant circuits may be employed in IPT systems to improve power transfer efficiency and extend the operating range.

Both the transmitter and receiver coils may be part of LC resonant circuits, where the inductance (L) of the coils and the capacitance (C) of associated capacitors are tuned to the same resonant frequency [1].

Custom Geometries and Integration:

Coils can be customized to fit specific form factors or spatial constraints of the devices involved. This may involve variations in coil size, shape, or winding patterns.

In some cases, coils may be integrated into the design of electronic devices or charging pads, allowing for seamless wireless charging without the need for external components.

Overall, the physical representation of IPT in WPT systems involves the careful design and arrangement of coils, along with considerations of core materials, resonant circuits, and integration with electronic devices. These elements work together to achieve efficient and reliable wireless power transfer in various applications.

1.4.2 Efficiency and Limitations of IPT

Inductive Power Transfer (IPT) offers several advantages, including wireless charging capabilities and convenience. However, it also has its limitations and efficiency considerations. Here's a breakdown:

Efficiency:

- **High Efficiency:** IPT systems can achieve high efficiency, especially when designed with resonant circuits. Resonant coupling allows for more efficient power transfer over longer distances compared to non-resonant systems. [1]
- **Resonant Coupling:** By utilizing resonance between the transmitter and receiver coils, IPT systems can achieve higher efficiency. Resonant coupling enables efficient power transfer even when the coils are not perfectly aligned, allowing for more flexibility in device placement [4].
- **Controlled Power Transfer:** IPT systems can regulate the power transfer process to optimize efficiency. Techniques such as impedance matching and adaptive tuning help ensure maximum power transfer under varying load conditions. [3]

- **Suitable for Various Applications:** IPT is suitable for various applications, including consumer electronics, electric vehicle charging, and medical devices, where wireless power transfer is desirable.

Limitations:

- **Distance Limitations:** While IPT systems can transfer power wirelessly, the distance over which efficient power transfer can occur is limited. The efficiency of power transfer decreases as the distance between the transmitter and receiver coils increases. Thus, for practical applications, IPT systems are typically designed for relatively short-range power transfer.
- **Alignment Sensitivity:** Non-resonant IPT systems are highly sensitive to the alignment between the transmitter and receiver coils. Misalignment can lead to reduced efficiency and power transfer. Although resonant systems offer improved tolerance to misalignment, proper alignment is still crucial for optimal performance.
- **Power Losses**: IPT systems may experience power losses due to factors such as resistive losses in the coils, core losses in magnetic materials, and electromagnetic interference. These losses can reduce the overall efficiency of the system.
- **Heat Generation**: Power transfer in IPT systems can generate heat, particularly in the coils and associated electronics. Heat dissipation becomes a concern, especially during high-power charging or prolonged operation, which can affect system efficiency and reliability.

In summary, while IPT systems offer high efficiency and convenient wireless charging capabilities, they also have limitations related to distance, alignment sensitivity, power losses, and heat generation. Understanding these efficiency considerations and limitations is essential for designing and deploying IPT systems in various applications effectively

1.5 Circuit Models and Topologies for Resonant WPT

Resonant WPT systems employ various circuit models and topologies to efficiently transfer electrical power wirelessly. Here are some common circuit models and topologies used in resonant WPT:

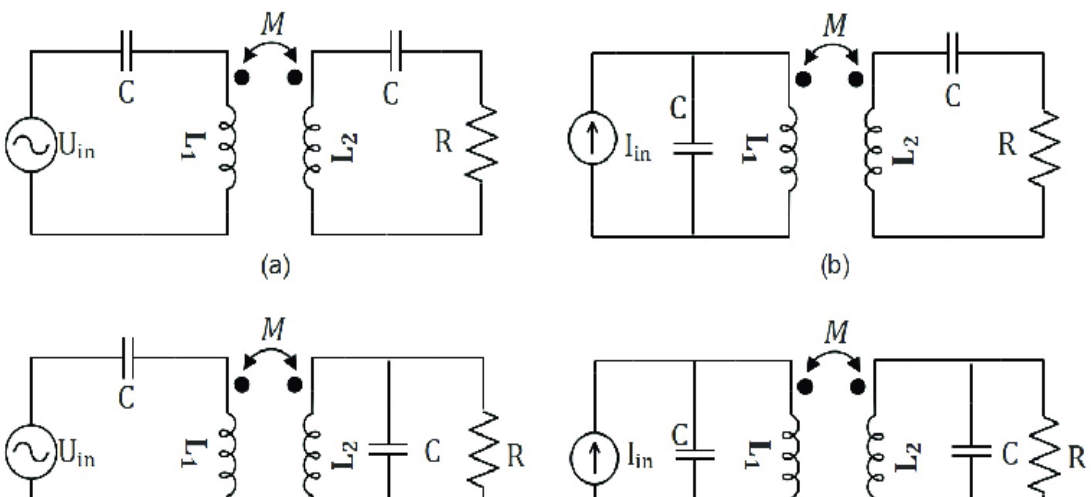

Figure 1-8 :Four Topologies for Resonant WPT

1.5.1 Series-Series Resonant Circuit Model for WPT

In the Series-Series (S-S) topology for resonant WPT, both the transmitter and receiver coils are connected in series. Each coil is also connected to a capacitor to form a resonant LC circuit. This topology allows for efficient power transfer over a short to medium range. Both transmitter and receiver coils are tuned to the same resonant frequency figure 1-8 (a) [7].

- ✓ **Applications:** S-S resonant WPT systems are suitable for applications where efficiency and moderate distance power transfer are required. They are commonly used in consumer electronics, medical devices, and automotive applications where close-range wireless charging is needed [7].
- ✓ **Advantages:**
  - Simplified circuit design compared to other topologies.
  - Good efficiency over moderate distances.
  - Can achieve high power transfer efficiency when properly tuned.
- ✓ **Disadvantages:**
  - Limited to short to medium-range power transfer due to the series connection.
  - Efficiency can decrease significantly with misalignment between coils.
  - Requires precise tuning of both transmitter and receiver coils for optimal performance.

1.5.2 Series-Parallel Resonant Circuit Model for WPT

The Series-Parallel (S-P) topology combines series and parallel connections of coils and capacitors, in the resonant circuit the transmitter coil (primary) is connected in series with a capacitor to form a resonant tank circuit, similar to the Series-Series configuration. However, on the receiver side, the coil (secondary) is connected in parallel with a capacitor, forming another resonant tank circuit figure 1-8 [7].

- ✓ **Applications:**

S-P resonant WPT systems are suitable for applications requiring efficient power transfer over a wider range of distances compared to Series-Series topology. They are commonly used in industrial

automation, electric vehicles, and wireless charging infrastructure where moderate to long-range power transfer is needed.

✓ **Advantages:**

- Better impedance matching compared to S-S topology, leading to improved efficiency.
- More flexibility in tuning and optimization of the resonant circuit for different distances.
- Higher tolerance to misalignment between transmitter and receiver coils.

✓ **Disadvantages:**

- Slightly more complex circuit design compared to S-S topology.
- May require additional components for impedance matching and tuning.

1.5.3 Parallel-Parallel Resonant Circuit Model for WPT

In the Parallel-Parallel (P-P) topology the transmitter coil (primary) is connected in parallel with a capacitor to form a resonant tank circuit. Similarly, the receiver coil (secondary) is connected in parallel with a capacitor to form another resonant tank circuit figure 1-8 (d) [7].

✓ **Applications:**

P-P resonant WPT systems are suitable for applications requiring efficient power transfer over short to moderate distances. They are commonly used in consumer electronics, IoT devices, and wearable technology where close-range wireless charging is needed.

✓ **Advantages:**

- Simplified circuit design compared to other topologies.
- Good efficiency over short to moderate distances.
- Can achieve high power transfer efficiency with proper tuning.

✓ **Disadvantages:**

- Limited to short to moderate-range power transfer due to the parallel connection.
- Efficiency may decrease significantly with misalignment between coils.
- May not be as efficient over longer distances compared to S-P or S-S topologies.

1.5.4 Parallel-Series Resonant Circuit Model for WPT

The Parallel-Series (P-S) topology combines parallel and series connections of coils and capacitors in the resonant circuit. In this topology, the transmitter coil (primary) is connected in parallel with a capacitor to form a resonant tank circuit. On the receiver side, the coil (secondary) is connected in series with a capacitor, forming another resonant tank circuit figure 1-8 (b). [7]

✓ **Applications:**

Parallel-Series resonant WPT systems are suitable for applications requiring efficient power transfer over a wide range of distances. They are commonly used in industrial automation, electric vehicle charging, and consumer electronics where flexibility in distance and efficiency are essential.

Advantages:

- Improved impedance matching compared to other topologies, leading to enhanced efficiency.
- Flexibility in tuning and optimization of the resonant circuit for different distances.
- Higher tolerance to misalignment between transmitter and receiver coils.

Disadvantages:

- May require more complex circuit design compared to other topologies.
- Additional components may be needed for impedance matching and tuning.

1.6 Mathematical Derivation of Resonance Condition

1.6.1.1 Series Type

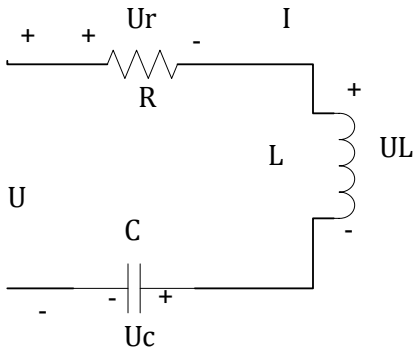

Figure 1-9 : Circuit diagram of series compensation circuit

In This RLC series circuit, as depicted in Figure 1.7, the total impedance Z_s can be inferred as

$$Zs = R + j\omega L + \frac{1}{jwC} = R + j\left(\omega L - \frac{1}{wC}\right) = R + jX \tag{1-1}$$

where X represents the imaginary component of the total equivalent impedance.When $X = 0$, the resonant angular frequency w_0 can be calculated as

$$w_0 = \frac{1}{\sqrt{wC}} \tag{1-2}$$

Subsequently, the resonance frequency is obtained as

$$f_0 = \frac{1}{2\pi\sqrt{LC}} \tag{1-3}$$

1.6.1.2 Parallel Type

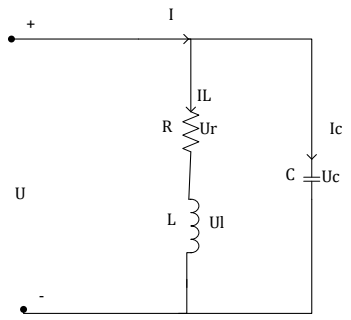

Figure 1-10: Circuit diagram of parallel compensation circuit

In practical IPT systems, the compensating capacitance is connected in parallel with the coils, where the coils possess inductance L and internal resistance R, as depicted in Figure 1-10, and the total impedance can be determined as

$$Z_p = \frac{(R + j\omega L)\frac{1}{j\omega C}}{R + j\omega L + \frac{1}{j\omega C}} \tag{1-4}$$

Let $Im\{Zp\} = 0$, the resonance angular frequency ω_0 can be obtained as

$$w_0 = \sqrt{\frac{1}{LC} - \frac{R^2}{L^2}} \tag{1-5}$$

can be derived when $R < \sqrt{\frac{L}{C}}$. Then, the resonance frequency is derived as

$$f_0 = \frac{1}{2\pi}\sqrt{\frac{1}{LC} - \frac{R^2}{L^2}} \tag{1-6}$$

1.6.2 Analysis of Series and Parallel Resonance Configurations

Series type

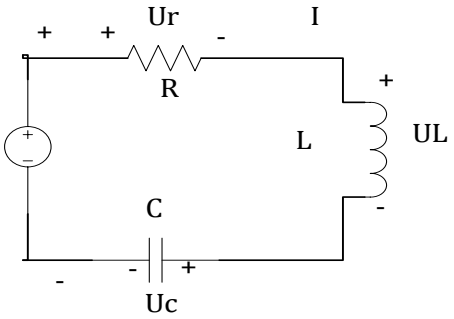

Figure 1-11Series RLC AC Circuits

$$Z_{in} = jwL + \frac{1}{jwL} + R \tag{1-7}$$

Complex power delivered to the resonator

$$P_i = \frac{1}{2} VI = \frac{1}{2} Z_{in} |I|^2 \left(R + jwL - j \frac{1}{wc}\right) \quad (1\text{-}8)$$

Power dissipated by the resistor R

$$P_l = \frac{1}{2} |I|^2 \mathrm{R} \quad (1\text{-}9)$$

Average magnetic energy stored in the inductor

$$W_m = \frac{1}{2} |I|^2 \mathrm{L} \quad (1\text{-}10)$$

Average electric energy stored in the capacitor

$$W_e = \frac{1}{4} |V_c|^2 \mathrm{C} = \frac{1}{4} |I|^2 \frac{1}{w^2 C} \quad (1\text{-}11)$$

Complex power rewritten in terms of energy stored and power dissipated

$$P_{in} = P_l + 2jw(W_m + W_e) \quad (1\text{-}12)$$

Input impedance rewritten in terms of energy stored and power dissipated

$$Z_{in} = \frac{2P_{in}}{|I|^2} = \frac{P_l + 2jw(W_m + W_e)}{\frac{1}{2}|I|^2} \quad (1\text{-}13)$$

At resonance we have that W_m=W_e so Z_{in} becomes

$$Z_{in} = \frac{2P_{in}}{|I|^2} = \mathrm{R} \quad (1\text{-}14)$$

And the resonance frequency is

$$w_0 = \frac{1}{\sqrt{LC}} \quad (1\text{-}15)$$

Parallel Type

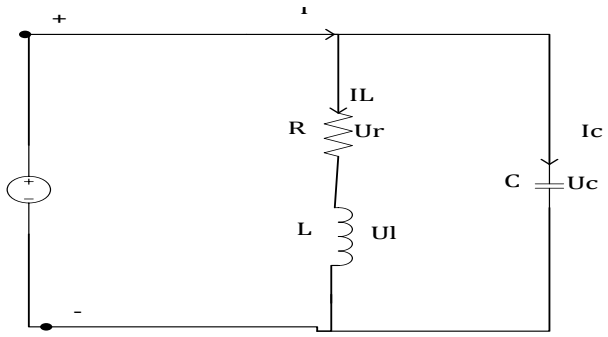

Figure 1-12 Parallel RLC AC Circuits

$$Z_{in} = \left(\frac{1}{R} + \frac{1}{jwL} + \text{jwC}\right)^{-1} \tag{1-16}$$

Complex power delivered to the resonator

$$P_i = \frac{1}{2} VI = \frac{1}{2} \frac{|V|^2}{Z_{in}} \left(\frac{1}{R} + \frac{j}{wL} - \text{jwC}\right) \tag{1-17}$$

Power dissipated by the resistor R

$$P_l = \frac{1}{2}\frac{|V|^2}{R} \tag{1-18}$$

Average magnetic energy stored in the inductor

$$W_m = \frac{1}{4}|I_L|^2\text{L} = \frac{1}{4}|V|^2\frac{1}{w^2L} \tag{1-19}$$

Average electric energy stored in the capacitor

$$W_e = \frac{1}{2}|V|^2\text{C} \tag{1-20}$$

Complex power rewritten in terms of energy stored and power dissipated

$$P_{in} = P_l + 2jw(W_m - W_e) \tag{1-21}$$

Input impedance rewritten in terms of energy stored and power dissipated

$$Z_{in} = \frac{2P_{in}}{|I|^2} = \frac{P_l + 2jw(W_m - W_e)}{\frac{1}{2}|I|^2} \tag{1-22}$$

At resonance we have that $W_m = W_e$ so Z_{in} becomes

$$Z_{in} = \frac{2P_{in}}{|I|^2} = \text{R} \tag{1-23}$$

And the resonance frequency is

$$w_0 = \frac{1}{\sqrt{LC}} \tag{1-24}$$

1.7 Impedance Matching and Maximum Power Transfer

1.7.1 Impedance Matching

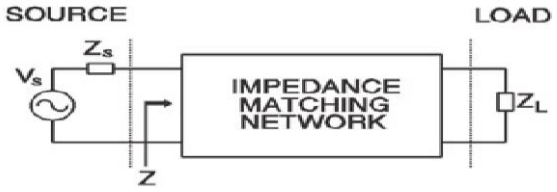

Figure 1-13Impedance Matching Networks for Wireless Applications

Impedance matching involves the process of aligning one impedance with another using circuit-based design methods, with the objective of achieving optimal system performance. This technology finds widespread application in transmission lines and is utilized across various fields including electrical engineering systems, acoustic systems, optical systems, and mechanical systems, all of which entail the transmission of energy from a source to a load. Typically, static impedance matching is implemented by designing a passive network between the source and the load, often referred to as a compensation network by some authors. Various components and circuits can be employed to achieve impedance matching.

In wireless power transfer (WPT) systems, two primary sources contributing to the degradation of system performance are frequency splitting and impedance mismatching. Frequency splitting arises from fluctuations in the coupling effect between transmitting and pickup coils. Impedance mismatching, on the other hand, quantifies differences in the input impedances of two circuits, potentially resulting in reflected signals from the receiver back into the transmitter, particularly in high-frequency transmission applications. In WPT systems, the necessity for impedance matching is underscored by

In this section, we delve into the theoretical analysis of a peer-to-peer system, focusing on the design of compensation networks. Our analysis emphasizes two key aspects: static impedance matching and adaptive impedance matching strategies. [1]

1.7.1.1 Maximum Power Transfer

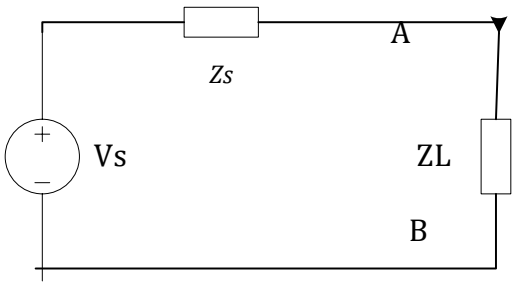

Figure 1-14Source and load impedance circuit

Suppose we have a voltage source V_S with a known, fixed, nonzero series source resistance $R_S > 0$. It's connected to a load which we're modeling as just a resistor.

We can solve this simple circuit by hand. The voltage source pushes current through a total resistance $R_S + R_L$. so the total current is

$$I_L = \frac{V_S}{R_S + R_L} \qquad (1\text{-}25)$$
$$V_L = I_L Z_L$$

We can solve this simple circuit by hand. The voltage source pushes current through a total resistance R_s+R_L, so the total current is

$$P_L = |I_L|^2 Re\{Z_L\} \qquad (1\text{-}26)$$
$$P_L = \frac{|V_S|^2 R_L}{(R_S + R_L)^2}$$

If V_S and R_S are fixed, then we're only looking at the behavior of the terms of the fraction involving R_L.

Look at the limits here:

1. **Load is short circuit.** If $R_L = 0$, then the numerator goes to zero, so $P(R_L) = 0$. No power is delivered if the load is a short circuit.
2. **Load is open circuit.** If $R_L = \infty$, then the numerator and denominator both go to infinity, but the denomniator has a squared term so it goes to infinity faster. that the fraction goes to 0, and $P(R_L) = 0$. No power is delivered if the load is an open circuit.
3. **Load is intermediate.** If our load resistance is somewhere $0 < R_L < \infty$, then there'll be some nonzero power $P(R_L) > 0$.

We can use calculus to find the maximum by solving for the value of RL that makes the derivative $dP(R_L)dR_L = 0$.

The result is that the maximum power occurs if $R_L = R_S$

At this maximum power point, the power transferred is:

$$P_L = \frac{{V_s}^2 R_S}{(R_S + R_L)^2} = \frac{{V_s}^2 R_S}{(2R_S)^2} = \frac{{V_s}^2}{4R_S} \qquad (1\text{-}27)$$

At this maximum power point, the same amount of power is dissipated in the load resistor and the source resistor:

$$P(VS) = P(RS) + P(RL) = \frac{{V_s}^2}{2R_S} \tag{1-28}$$

Note that this is the same as the power supplied by a voltage source connected to a single equivalent resistor of $R_{eq} = 2R_s$

1.7.2 Design Considerations for Resonant WPT Circuits

WPT using resonant circuits is a widely researched area with applications ranging from consumer electronics to electric vehicles. Here are some key design considerations for resonant WPT circuits:

1) **Frequency Selection:** Resonant WPT systems typically operate at high frequencies, often in the range of tens to hundreds of KHz or even MHZ. The selection of the operating frequency is crucial as it affects efficiency, coil size, and system complexity. Common choices include the low-frequency range (LF, 30 kHz - 300 kHz), the high-frequency range (HF, 3 MHz - 30 MHz), or the microwave range ($> 300\ MHz$) [1].
2) **Resonant Topology Selection:** There are various resonant topologies used in WPT systems such as series LC, parallel LC, or series-parallel hybrid resonant circuits. Each has its advantages and disadvantages in terms of efficiency, coil design, and tolerance to load variations [7].
3) **Coil Design:** The design of the transmitter and receiver coils is critical for efficient power transfer. Coil geometry, number of turns, wire gauge, and core material all impact the efficiency and performance of the WPT system. Coupling coefficient between the transmitter and receiver coils should also be optimized for maximum power transfer [7].
4) **Resonant Capacitors and Inductors:** Selection of high-quality capacitors and inductors with low losses is essential to minimize power dissipation and maximize efficiency. Capacitors and inductors should be chosen to have low equivalent series resistance (ESR) and equivalent series inductance (ESL) at the operating frequency [9].
5) **Impedance Matching:** Impedance matching between the transmitter and receiver circuits is crucial for efficient power transfer. Matching networks, such as L-section or T-section impedance matching circuits, can be employed to ensure maximum power transfer from the transmitter to the receiver [1].
6) **Control and Regulation:** Implementing control and regulation techniques is necessary to maintain stable power transfer and ensure efficiency. This may include feedback loops for automatic frequency tuning, or power regulation based on load conditions.
7) **Safety Considerations:** Safety is paramount in WPT systems to prevent electromagnetic interference (EMI) and ensure user safety. Shielding, isolation techniques, and compliance

with regulatory standards such as FCC regulations for electromagnetic radiation are essential.

8) **Efficiency Optimization:** Maximizing efficiency is a key design goal for resonant WPT systems. This involves minimizing losses in the transmitter and receiver circuits, optimizing coil design and placement, and reducing parasitic capacitances and resistances [3].
9) **Foreign Object Detection (FOD):** Implementing FOD mechanisms is crucial to prevent accidental power transfer to metallic objects or other foreign objects that may come into proximity with the WPT system. This typically involves using sensors or monitoring techniques to detect foreign objects and shutting down the power transfer process if detected.
10) **Scalability and Flexibility:** Designing WPT systems with scalability and flexibility in mind allows for easy integration into various applications and environments. This includes considering factors such as power levels, distance of power transfer, and compatibility with different receiver devices.

1.8 Overview of Dynamic Wireless Power Transfer (DWC)

Transmission of power without wires for supplying power to electrical devices and equipment,and for charging has been contemplated since the times of Tesla. However, this was not possibleat that time because associated enabling technologies were not available. A breakthrough to thisend was achieved in 2007 when researchers lit up a bulb from a wireless power source at a distance of two metres . Much advancement in this field has been made since this major success [10]

Dynamic Wireless Power Transfer (DWPT) or Dynamic Wireless Charging (DWC) is a technology that enables electric vehicles (EVs) to charge wirelessly while on the move. Unlike traditional EV charging methods that require a physical connection between the vehicle and a charging station, DWC uses electromagnetic fields to transfer power from the charging infrastructure to the vehicle's battery.

DWPT systems typically consist of two main components: the charging infrastructure embeddedbin the road or a charging track, and a receiving coil installed on the EV. The charging infrastructure generates a magnetic field, which induces a current in the receiving coil, thereby charging the EV's battery.

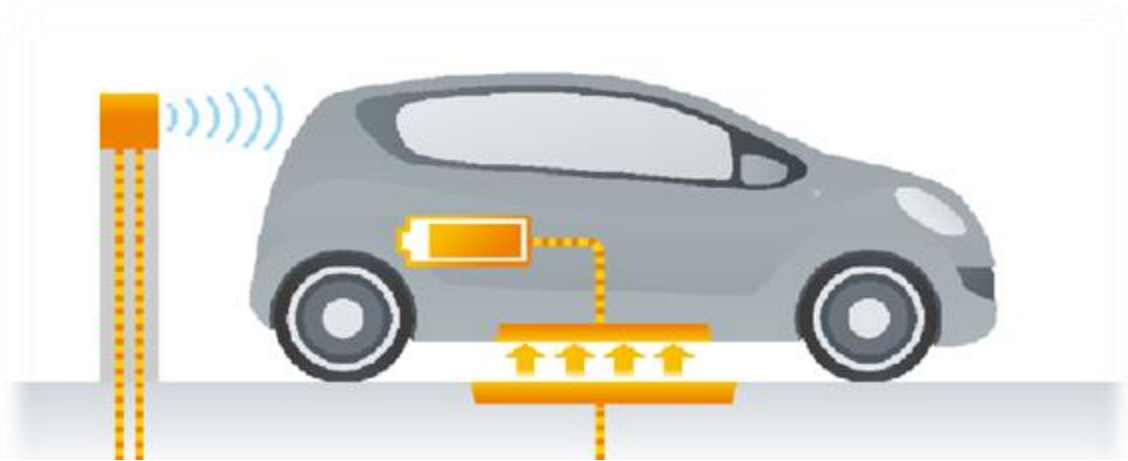

Figure 1-15: Drawing representing wireless car charging.

1.8.1 Concept and Operational Principles of DWC

The development of pure battery electric vehicle (EV) and plug-in hybrid electric vehicle (PHEV) markets demands more recharging facilities on recharging. The WPT technologies are emerging, safe, convenient, flexible and autonomous charging methods for both EVs and PHEVs [11]

The WPT technologies use electromagnetic field, or electric filed, or mechanical force to transfer energy from the electricity grid to onboard battery chargers in close proximity. The EV is inherently isolated from the utility's grid but via the air gap between WPT transmitting pad and EV-mounted receiving coil. WPT charging is also convenient and flexible since no cables and connectors are required and wireless charging becomes fully autonomous. Automotive manufacturers and major global automobile suppliers have commenced R&D work on different WPT technologies.

dynamic wireless charging (DWC) is a technology that allows electric vehicles (EVs) to charge while in motion, without the need for physical cables or plugs.

Principles:

Basic Operating principle

Figure 1-16 Basic block diagram of static wireless charging system for EVs depicts the elemental diagram of the static WCS for EVs. To facilitate power transfer from the transmission coil to the receiving coil, the grid's electricity (AC) is converted to high frequency (HF) AC (AC) through AC/DC and DC/AC converters. On both the transmitting and receiving sides, compensatory topologies supported series and parallel combinations are wont to increase overall system efficiency. The receiving coil, which is typically placed underneath the vehicle, transforms the oscillating magnetic flux fields to high-frequency electricity (HFAC). The high-frequency electricity is then transformed to a gradual DC supply hats utilized to power the on-board batteries. to stop any health and safety concerns and to ensure steady operation, the facility control, communications, and battery management system (BMS) also are incorporated.

Magnetic planar ferrite plates are used on both the transmitter and receiver sides to attenuate detrimental leakage fluxes and enhance magnetic flux distribution.

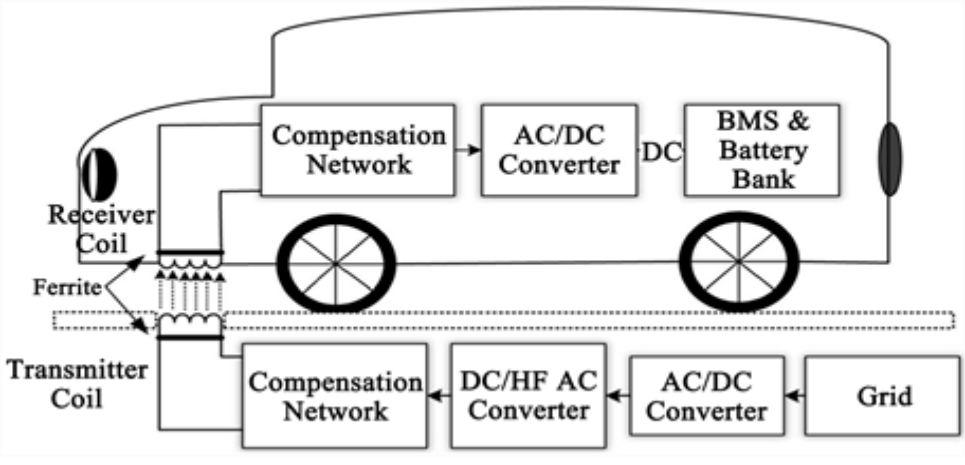

Figure 1-16 Basic block diagram of static wireless charging system for EVs

1.8.2 Applications and Benefits of DWC for Electric Vehicles (EVs)

Applications

An application for dynamic wireless charging (DWC) for electric vehicles (EVs) could be

designed to provide real-time information and control over the charging process

Here's a conceptual outline for such an application in Dynamic Wireless Charging Control System for Electric Vehicles

Features:

- **Real-time Monitoring:** Users can monitor the charging status of their EVs, including current charge level, charging rate, and estimated time to full charge.
- **Charging Schedule:** Users can set a charging schedule based on their daily routines or preferences. The application can optimize charging times to take advantage of off-peak electricity rates.
- **Route Planning:** The application can suggest optimal routes that include DWC infrastructure, ensuring continuous charging during long trips.
- **Energy Management:** Users can manage energy consumption and set limits to avoid overcharging or excessive discharge of the battery.
- **Notifications:** The application can send notifications about charging status, reminders for scheduled charging, and alerts for any issues or maintenance requirements.
- **Integration with Smart Grids:** The application can communicate with smart grids to optimize charging based on renewable energy availability and grid load.
- **User Profile**: Users can create profiles for multiple vehicles, allowing them to manage and monitor charging for their entire fleet.
- **Payment Integration:** The application can facilitate payment for charging services, either through a subscription model or pay-as-you-go.

Benefits:

- **Convenience:** Users can manage their EV charging remotely, reducing the need for manual intervention.

- **Efficiency:** Optimal charging schedules and energy management help reduce energy costs and increase battery lifespan.
- **Environmental Impact:** By encouraging the use of renewable energy sources, the application can contribute to reducing carbon emissions.

1.8.3 System Architecture for Dynamic Charging of EVs

Each vehicle contains a pick-up device, battery, regulator, and motor. A charging unit is a power track, which consists of an inverter and an inductive track. In the OLEV system, 60 Hz power supplied from the public electric grid is converted to a frequency of 20 kHz through the inverter. From the inverter, a high current flow through the coiled inductive track placed beneath the road. The high current induces a magnetic flux toward a surface of the road and the magnetic flux is transmitted to the bottom of the vehicle while the vehicle passes over. The power is then generated by converting the electromagnetic field into current at the pick-up device. The remotely collected electricity is distributed to the motor, to the battery via the regulator, or both, depending on the power requirement of the motor and the battery's energy level. The more detailed system architecture can be found in [12] [13]

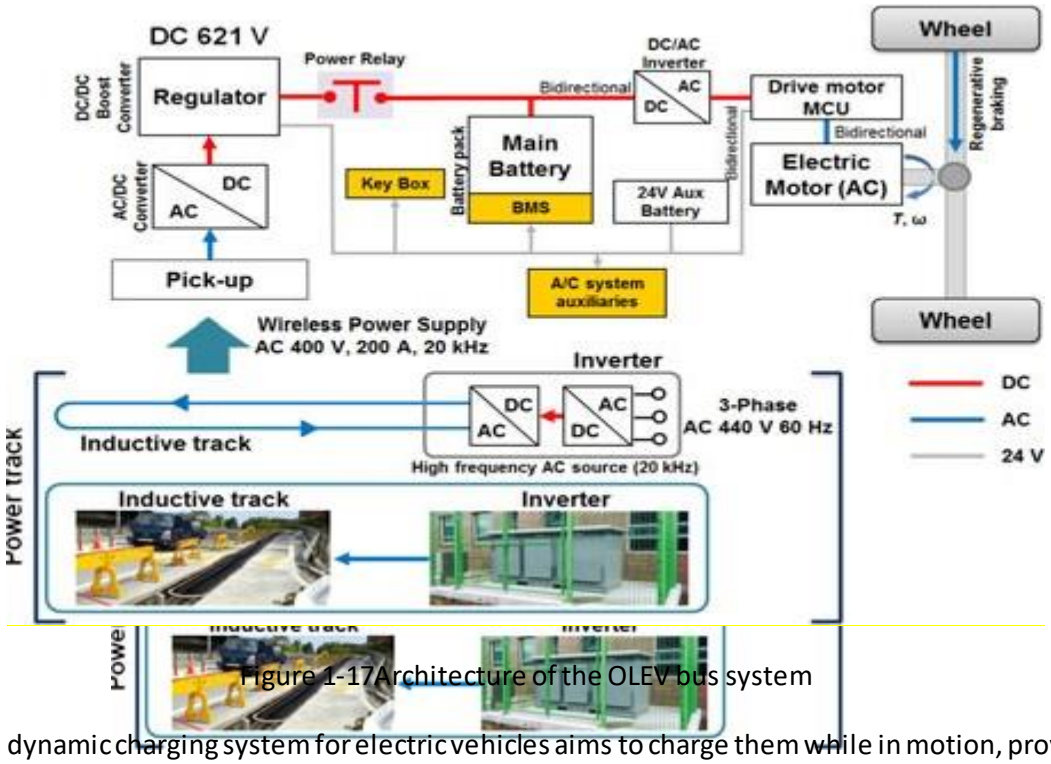

Figure 1-17Architecture of the OLEV bus system

So, the dynamic charging system for electric vehicles aims to charge them while in motion, providing significant convenience for electric vehicle owners and contributing to their sustainability. This system relies on wireless charging technologies, where power is transferred from an external source to the vehicle through methods such as electromagnetic resonance or inductive charging. Its engineering includes several key components such as the power source, power conversion system, vehicle receiver, battery management, and other elements that ensure efficient charging and vehicle safety. The integration of these components allows for continuous charging while the vehicle is in use, enhancing the electric driving experience and contributing to the development of future wireless charging technologies.

1.9 Conclusion

Wireless power technology offers the promise of cutting the last cord, allowing users to seamlessly recharge mobile devices as easily as data are transmitted through the air. Initial work on the use of magnetically coupled resonators for this purpose has shown promising results. We present new analysis that yields critical insight into the design of practical systems, including the introduction of key figures of merit that can be used to compare systems with vastly different geometries and operating conditions.

Chaptre 2: Design and modeling of WPT systems

2.1 Block Diagram of typical WPT

The figure 2.1illustrates a block diagram of an Inductive Power Transfer (IPT) system utilizing magnetic resonant coupling [14]. This system facilitates wireless power transfer by eliminating physical connectors and enhancing convenience and flexibility. It comprises three main sections:

1) **High-Frequency Power Terminal:**
   - Power Supply: Provides electrical energy.
   - Inverter: Converts input power into high-frequency AC.
2) **Coupling Circuit:**
   - Transmitting Coil: Generates a magnetic field.
   - Pickup Coil: Induces voltage via magnetic resonance across an air gap.
3) **Load-Receiving Terminal:**
   - Rectifier: Converts high-frequency AC to DC.
   - Load: Receives the transmitted energy.

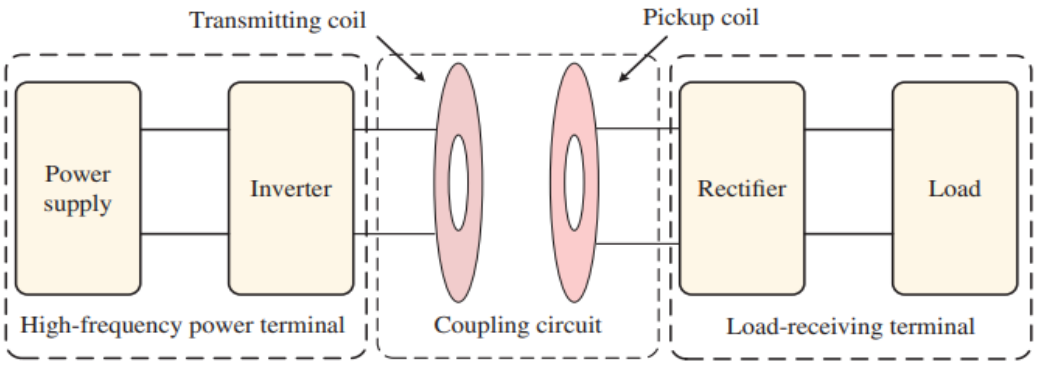

Figure 2-1: Block Diagram of Wireless Power Transmission

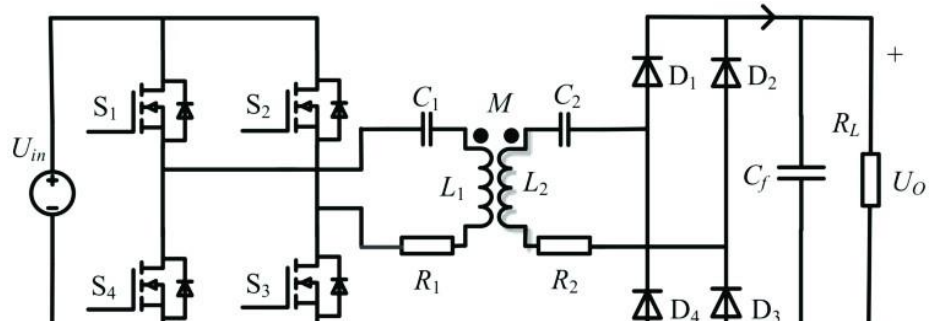

Figure 2-2: Circuit Diagram of WPT system

Figure 2.2 shows the circuit diagram of the main sections.

A typical circuit diagram for a WPT system includes:

Transmitter side:

DC input voltage (U_{in})

MOSFETs ($S_1 - S_2 - S_3 - S_4$) for switching

Inductors (L_1, L_2) are used to enhance the magnetic coupling between the transmitter and receiver coils

Capacitors ($C1, C2$) are used to regulate the voltage and stabilize the system by filtering out noise and smoothing the output voltage.

Receiver side:

Rectifier diodes ($D_1 - D_2 - D_3 - D_4$)

Filter capacitor (C_f)

Load resistor (R) is charged with a power

2.2 Modeling of WPT Systems

2.2.1 Analytical modeling

The circuit depicted in Figure 2.2 comprises five reactive components, which are described by five equations. These equations stem from the assumptions of ideal components, fixed parameters, and resonance conditions [15].

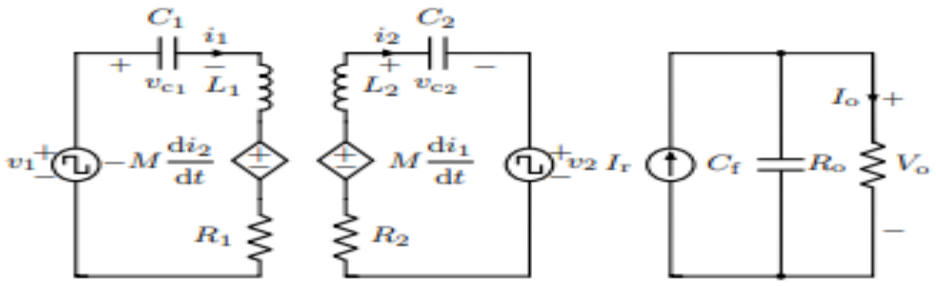

Figure 2-3: Circuit topology for WPT under consideration.

Ideal components with no parasitic resistances, inductances, capacitances, or forward voltages are assumed. Additionally, fixed parameters such as switching frequency, phase shift, and dead band, along with the assumption of resonance, are considered constants in the analysis.

$$\begin{aligned} L_1 \frac{\mathrm{d}i_1}{\mathrm{d}t} &= v_1 - v_{\mathrm{c}_1} + M \frac{\mathrm{d}i_2}{\mathrm{d}t} - i_1 R_1 \\ L_2 \frac{\mathrm{d}i_2}{\mathrm{d}t} &= M \frac{\mathrm{d}i_1}{\mathrm{d}t} - v_{\mathrm{c}_2} - v_2 - i_2 R_2 \\ C_1 \frac{\mathrm{d}v_{c_1}}{\mathrm{d}t} &= i_1 \\ C_2 \frac{\mathrm{d}v_{c_2}}{\mathrm{d}t} &= i_2 \\ C_{\mathrm{f}} \frac{\mathrm{d}V_{\mathrm{o}}}{\mathrm{d}t} &= I_{\mathrm{r}} - \frac{V_{\mathrm{o}}}{R_{\mathrm{o}}}. \end{aligned} \tag{2-1}$$

The initial four equations describe the behavior of the resonant tank under AC conditions, while the final equation represents the output filter under DC conditions. The combination of AC and DC signals complicates the theoretical analysis, thus requiring conversion to pure DC equations for simplification [15]

2.2.1.1 Large-Signal Model

The WPT system depicted in Figure 2.2 Bearing this in mind and according to [12], [41], a signal in the resonant tank can be decomposed as a sum of d-axis and q-axis components, From this point of view, the AC signals in the resonant tank can be approximated by their first harmonic without leading to a substantial loss in the accuracy [15].

$$\begin{aligned} v_1 &\approx V_{1d} sin(\omega_s t) + V_{1q} cos(\omega_s t) \\ i_1 &\approx I_{1d} sin(\omega_s t) + I_{1q} cos(\omega_s t) \end{aligned} \tag{2-2}$$

The AC signals in the receiving resonator can be broken down similarly. Consider the nonlinear sources v_1, v_2, and I_r. To derive analytical expressions [15]:

1) v_1 can be represented as the difference between voltages v_a and v_b, where v_a and v_b are square waves with amplitudes switching between 0 and V_d (voltage of the DC source). v_b has a phase lag of -π-α compared to v_a, where α is the phase shift between leading and lagging legs. Assuming v_a and v_b have phases of $\frac{\alpha}{2}$ and $\frac{-\pi-\alpha}{2}$ respectively, the first harmonic approximation of v_1 can be expressed as [15]:

$$\begin{aligned} v_1 &= v_a - v_b \\ &\approx \frac{2V_d}{\pi}\left(sin\left(\omega_s t + \frac{\alpha}{2}\right) - sin\left(\omega_s t - \pi - \frac{\alpha}{2}\right)\right) \\ &= \frac{4V_d}{\pi} cos\left(\frac{\alpha}{2}\right) sin(\omega_s t) \end{aligned} \tag{2-3}$$

showing that

$$V_{1d} = \frac{1V_d}{\pi} cos\left(\frac{\alpha}{2}\right), \qquad V_{1q} = 0. \tag{2-4}$$

2) Due to the clamping effect of the rectifier bridge, v_2 is a square wave with amplitude switching between $\pm V_o$ and has the same sign than i_2, $v_2 = sgn(i_2)V_o$. Meanwhile, since i_2 is very close to a sinusoid of frequency ω_s, the first harmonic approximation of v_2 can be defined in terms of i_2 [15].

$$v_2 = sgn(i_2)V_o \approx \frac{1V_o}{\pi}\frac{i_2}{\|i_2\|} = \frac{4V_o}{\pi}\frac{1}{\|i_2\|}\left(I_{2d}sin(\omega_s t) + I_{2q}cos(\omega_s t)\right) \quad (2\text{-}5)$$

where

$$\|i_2\| = \sqrt{I_{2d}^2 + I_{2q}^2} \quad (2\text{-}6)$$

It is then clear that

$$\left[V_{2d}, V_{2q}\right] = \frac{1V_o}{\pi\sqrt{I_{2d}^2 + I_{2q}^2}}\left[I_{2d}, I_{2q}\right] \quad (2\text{-}7)$$

When ideal rectifiers are taken into account, by the law of energy conservation, I_r equals the mean value of $|i_2|$. If we denote Ts as $\frac{2\pi}{\omega s}$, then: [15]

$$I_r = \frac{1}{T_s}\int_0^{T_s}|i_2|dt = \frac{\|i_2\|}{T_s}\int_0^{T_s}|sin(\omega_s t)|dt = \frac{2}{\pi}\sqrt{I_{2d}^2 + I_{2q}^2}. \quad (2\text{-}8)$$

Subsequently, by substituting equations (2-2) to (2-8) into (2-1), the d- and q-components are separated as follows [15]

$$
\begin{aligned}
\frac{dI_{1d}}{dt} &= \omega_s I_{1q} + \Upsilon_1\left(V_{1d} - V_{c_1 d} - I_{1d}R_1\right) \\
&\quad -\Upsilon_2\left(\Upsilon_4 I_{2d} + V_{c_2 d} + I_{2d}R_2\right) \\
\frac{dI_{2d}}{dt} &= \omega_s I_{2q} + \Upsilon_2\left(V_{1d} - V_{c_1 d} - I_{1d}R_1\right) \\
&\quad -\Upsilon_3\left(\Upsilon_4 I_{2d} + V_{c_2 d} + I_{2d}R_2\right) \\
\frac{dV_{c_1 d}}{dt} &= \omega_s V_{c_1 q} + \frac{1}{C_1} I_{1d} \\
\frac{dV_{c_2 d}}{dt} &= \omega_s V_{c_2 q} + \frac{1}{C_2} I_{2d} \\
\frac{dI_{1q}}{dt} &= -\omega_s I_{1d} - \Upsilon_1\left(V_{c_1 q} + I_{1q}R_1\right) \\
&\quad -\Upsilon_2\left(\Upsilon_4 I_{2q} + V_{c_2 q} + I_{2q}R_2\right) \\
\frac{dI_{2q}}{dt} &= -\omega_s I_{2d} - \Upsilon_2\left(V_{c_1 q} + I_{1q}R_1\right) \\
&\quad -\Upsilon_3\left(\Upsilon_4 I_{2q} + V_{c_2 q} + I_{2q}R_2\right) \\
\frac{dV_{c_1 q}}{dt} &= -\omega_s V_{c_1 d} + \frac{1}{C_1} I_{1q} \\
\frac{dV_{c_2 q}}{dt} &= -\omega_s V_{c_2 d} + \frac{1}{C_2} I_{2q} \\
\frac{dV_o}{dt} &= \frac{1}{C_f}\left(I_r - \frac{V_o}{R_o}\right).
\end{aligned}
\tag{2-9}
$$

where

$$
\begin{aligned}
[\Upsilon_1, \Upsilon_2, \Upsilon_3] &= \frac{1}{L_1 L_2 - M^2}[L_2, M, L_1] \\
\Upsilon_4 &= \frac{4V_o}{\pi\sqrt{I_{2d}^2 + I_{2q}^2}}.
\end{aligned}
\tag{2-10}
$$

Equation (2-9) represents the large-signal model, which can be transformed into an equivalent state-space form. [15]

$$
\begin{cases}
\dfrac{d\boldsymbol{X}(t)}{dt} = \boldsymbol{A}\boldsymbol{X}(t) + \boldsymbol{B} \\
V_o(t) = \boldsymbol{C}\boldsymbol{X}(t)
\end{cases}
\tag{2-11}
$$

In this context, the system matrices {**A**, **B**, **C**} and the state vector $\boldsymbol{X}(t)$ are defined as follows: [15]

$$\mathbf{A}=\begin{bmatrix} -\Upsilon_1 R_1 & -\Upsilon_2(\Upsilon_4+R_2) & -\Upsilon_1 & -\Upsilon_2 & \omega_s & 0 & 0 & 0 & 0 \\ -\Upsilon_2 R_1 & -\Upsilon_3(\Upsilon_4+R_2) & -\Upsilon_2 & -\Upsilon_3 & 0 & \omega_s & 0 & 0 & 0 \\ 1/C_1 & 0 & 0 & 0 & 0 & 0 & \omega_s & 0 & 0 \\ 0 & 1/C_2 & 0 & 0 & 0 & 0 & 0 & \omega_s & 0 \\ -\omega_s & 0 & 0 & 0 & -\Upsilon_1 R_1 & -\Upsilon_2(\Upsilon_4+R_2) & -\Upsilon_1 & -\Upsilon_2 & 0 \\ 0 & -\omega_s & 0 & 0 & -\Upsilon_2 R_1 & -\Upsilon_3(\Upsilon_4+R_2) & -\Upsilon_2 & -\Upsilon_3 & 0 \\ 0 & 0 & -\omega_s & 0 & 1/C_1 & 0 & 0 & 0 & 0 \\ 0 & 0 & 0 & -\omega_s & 0 & 1/C_2 & 0 & 0 & 0 \\ 0 & 0 & 0 & 0 & 0 & 0 & 0 & 0 & -1/(C_f R_o) \end{bmatrix} \quad (2\text{-}12)$$

$$\mathbf{B}=[\Upsilon_1 V_{1d}, \Upsilon_2 V_{1d}, 0,0,0,0,0, I_r/C_f]^\top$$

$$C=[0,0,0,0,0,0,0,0,1]$$

$$\mathbf{X}(t)=\left[I_{1d}(t), I_{2d}(t), V_{c_1 d}(t), V_{c_2 \mathbf{d}}(t), I_{1q}(t), I_{2q}(t), V_{c_1 \mathbf{q}}(t), V_{c_2 \mathbf{q}}(t), V_o(t)\right]^\top$$

$$\boldsymbol{F}=\begin{bmatrix} -\Upsilon_1 R_1 & -\Upsilon_2(\Upsilon_{10}+R_2-\Upsilon_5) & -\Upsilon_1 & -\Upsilon_2 & \omega_s & \Upsilon_2\Upsilon_6 & 0 & 0 & -\Upsilon_2\Upsilon_8 \\ -\Upsilon_2 R_1 & -\Upsilon_3(\Upsilon_{10}+R_2-\Upsilon_5) & -\Upsilon_2 & -\Upsilon_3 & 0 & \omega_s+\Upsilon_3\Upsilon_6 & 0 & 0 & -\Upsilon_3\Upsilon_8 \\ \frac{1}{C_1} & 0 & 0 & 0 & 0 & 0 & \omega_s & 0 & 0 \\ 0 & \frac{1}{C_2} & 0 & 0 & 0 & 0 & 0 & \omega_s & 0 \\ -\omega_s & \Upsilon_2\Upsilon_6 & 0 & 0 & -\Upsilon_1 R_1 & -\Upsilon_2(\Upsilon_{10}+R_2-\Upsilon_7) & -\Upsilon_1 & -\Upsilon_2 & -\Upsilon_2\Upsilon_9 \\ 0 & -\omega_s+\Upsilon_3\Upsilon_6 & 0 & 0 & -\Upsilon_2 R_1 & -\Upsilon_3(\Upsilon_{10}+R_2-\Upsilon_7) & -\Upsilon_2 & -\Upsilon_3 & -\Upsilon_3\Upsilon_9 \\ 0 & 0 & -\omega_s & 0 & \frac{1}{C_1} & 0 & 0 & 0 & 0 \\ 0 & 0 & 0 & -\omega_s & 0 & \frac{1}{C_2} & 0 & 0 & 0 \\ 0 & \frac{\Upsilon_8}{(2C_4)} & 0 & 0 & 0 & \frac{\Upsilon_9}{(2C_f)} & 0 & 0 & -\frac{1}{(C_f R_o)} \end{bmatrix} \quad (2\text{-}13)$$

$$\boldsymbol{G}=[-\Upsilon_1\Upsilon_{11}, -\Upsilon_2\Upsilon_{11}, 0,0,0,0,0,0,0]^\top$$

$$\boldsymbol{H}=[0,0,0,0,0,0,0,0,1]$$

$$\tilde{\boldsymbol{x}}(t)=\left[\tilde{\imath}_{1d}(t), \tilde{\imath}_{2d}(t), \tilde{v}_{c_1 d}(t), \tilde{v}_{c_2 d}(t), \tilde{\imath}_{1q}(t), \tilde{\imath}_{2q}(t), \tilde{v}_{c_1 q}(t), \tilde{v}_{c_2 q}(t), \tilde{v}_o(t)\right]^\top$$

2.2.1.2 Small-Signal Model

Due to the nonlinear relationship between V1d and α, see (4), the large-signal model (10) cannot be written in input output form necessary for control design. Therefore, the large signal model needs to be linearized around some static point to obtain a small-signal model that is linear in the variables. To this end, all the signals in the circuit should be decomposed as a static value plus a small signal, $V_0 = \bar{V}_0 + \tilde{V}_0$, where $\bar{V}_o$ and $\tilde{v}_0$ denote the static and small-signal parts, respectively. [15]

$$\begin{aligned} \tilde{v}_{1d} &\approx -\Upsilon_{11}\tilde{\alpha} \\ \tilde{v}_{2d} &\approx (\Upsilon_{10}-\Upsilon_5)\tilde{\imath}_{2d} - \Upsilon_6\tilde{\imath}_{2q} + \Upsilon_8\tilde{v}_o \\ \tilde{v}_{2q} &\approx (\Upsilon_{10}-\Upsilon_7)\tilde{\imath}_{2q} - \Upsilon_6\tilde{\imath}_{2d} + \Upsilon_9\tilde{v}_o \\ \tilde{\imath}_r &\approx \frac{1}{2}\left(\Upsilon_8\tilde{\imath}_{2d} + \Upsilon_9\tilde{\imath}_{2q}\right) \end{aligned} \quad (2\text{-}14)$$

Where

$$[\Upsilon_5, \Upsilon_6, \Upsilon_7] = \frac{4\bar{V}_o}{\pi\sqrt{\left(\bar{I}_{2d}^2 + \bar{I}_{2q}^2\right)^3}}\left[\bar{I}_{2d}^2, \bar{I}_{2d}\bar{I}_{2q}, \bar{I}_{2q}^2\right] \tag{2-15}$$

$$[\Upsilon_8, \Upsilon_9, \Upsilon_{10}] = \frac{4}{\pi\sqrt{\bar{I}_{2d}^2 + \bar{I}_{2q}^2}}\left[\bar{I}_{2d}, \bar{I}_{2q}, \bar{V}_o\right] \tag{2-16}$$

$$\Upsilon_{11} = \frac{2V_d}{\pi} sin\left(\frac{\bar{\alpha}}{2}\right).$$

Subtracting static components from equations like (2-9) and (2-11) yields the small-signal state-space model [15]

$$\begin{cases} \dfrac{d\tilde{\boldsymbol{x}}(t)}{dt} = \boldsymbol{F}\tilde{\boldsymbol{x}}(t) + \boldsymbol{G}\tilde{\alpha}(t) \\ \bar{v}_o(t) = \boldsymbol{H}\tilde{\boldsymbol{x}}(t) \end{cases} \tag{2-17}$$

where {F, G, H} and $\tilde{\mathbf{x}}(t)$ are defined in (2-13).

2.3 System Efficiency

At steady state, the efficiency of the system is defined in terms of input power and output power [3] .

$$\eta = \frac{P_o}{P_{\text{in}}} = \frac{V_o I_o}{V_{\text{in}} I_{\text{in}}} \tag{2-18}$$

where I_{in} is the DC input current and I_o is the DC output current. Since all power losses are included in the equivalent series resistances (ESR), we can easily calculate efficiency using a basic equivalent circuit [3]. The result is given by

$$\eta = \frac{\text{Re}\left[-\dot{U}_o \dot{I}_2^*\right]}{\text{Re}\left[\dot{U}_{\text{in}} \dot{I}_1^*\right]} \tag{2-19}$$

Here, the system efficiency is also calculated as a function of coupling coefficient and load resistance, it shows that efficiency decreases as the coupling becomes weaker. For a fixed coupling coefficient, there is a corresponding load resistor that achieves maximum efficiency [3].

2.3.1 Maximum Efficiency Point Tracking (MEPT)

his circuit model is shown in Figure 2-4, where L1, C1, R1, L2, C2, and R2 are the inductance, capacitance, and equivalent series resistance (ESR) of the resonators on both sides, respectively, M is the mutual inductance of the coupled coils, U1 is the fundamental component of the driving voltage, and Re is the equivalent load resistance. Assume that the angular frequency of U1 is ω_s, and the angular resonance frequencies of the resonators on both sides are ω_1 and ω_2, respectively. When the system is tuned to resonance

$$w_s = w_1 = w_2$$

frequency division, quality factor and optimal load based on coupling mode theory were proposed

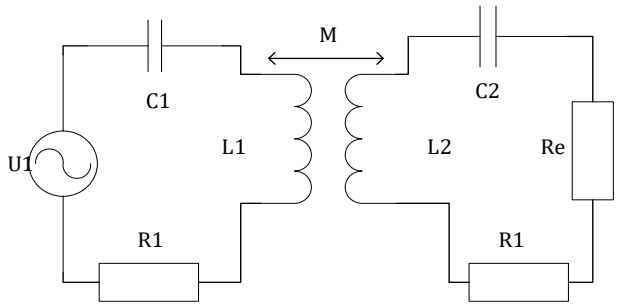

Figure 2-4 : Lumped parameter ac equivalent circuit model

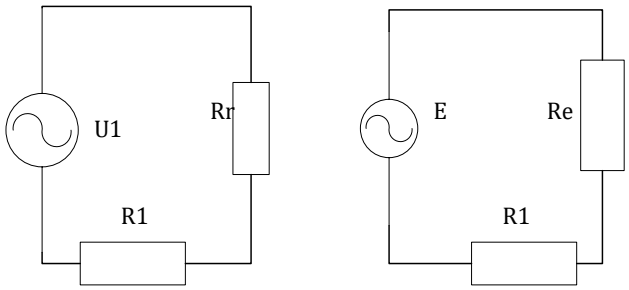

Figure 2-5: Decoupled ac equivalent circuit

Figure 2-4 can be decoupled as Figure 2-5, where E is the induced voltage, and Rr is the reflected resistance:

$$\begin{cases} Z_p = R_1 + j\left(\omega L_1 - \dfrac{1}{\omega C_1}\right) \\ Z_s = R_e + R_1 + j\left(\omega L_2 - \dfrac{1}{\omega C_e}\right) \end{cases} \quad 2\text{-}20)$$

$$Z_r = \frac{\omega^2 M^2}{Z_s} \quad 2\text{-}21)$$

where Z_p and Z_s are the primary and secondary equivalent impedances respectively

Regarding the transmission efficiency of the WPT system, the efficiency in the equivalent primary circuit and the efficiency in the secondary circuit, the so-called SS topology, can be calculated as follows

$$\begin{cases} \eta_p = \dfrac{Z_r}{R_1 + Z_r} \\ \eta_s = \dfrac{R_L}{R_2 + R_e} \end{cases} \quad (2\text{-}22)$$

The power transfer efficiency η is the product of the transmitting efficiency η_p and the receiving efficiency η_s

$$\eta = \eta_p \eta_s = \frac{\omega^2 \kappa^2 L_1 L_2 R_e}{(R_e + R_s)^2 R_p + \omega^2 \kappa^2 L_p L_s (R_L + R_s)} \quad (2\text{-}23)$$

By solving the derivative equation $\frac{\partial \eta}{\partial R_L} = 0$, the best equivalent value of $R_{L\eta max}$ to maximum transmission efficiency can be derived as

$$R_{L\eta max} = R_2\sqrt{1+\chi^2} \tag{2-24}$$

where Q_1 and Q_2 are the quality factors and κ is coupling coefficient. The maximum theoretical efficiency is given by:

$$\chi = \frac{\omega_s M}{\sqrt{R_1 R_2}} = \kappa\sqrt{Q_1 Q_2} \tag{2-25}$$

The maximal practical effectiveness is defined as:

$$\eta_{max} = 1 - \frac{2}{1+\sqrt{1+\chi^2}} \tag{2-26}$$

When χ is large, (2-24) can be approximated to:

$$\eta_{max} \approx \frac{\chi - 1}{\chi + 1} \tag{2-27}$$

The relationship between η_{max} and χ is shown by [16]

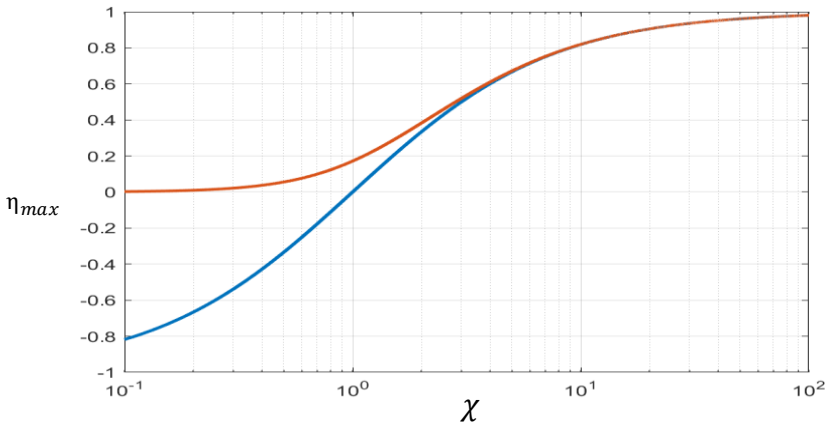

Figure 2-6: max system efficiency

According to (2-24) and (2-23) the optimal equivalent load resistance $R_{L\eta max}$ is a function of the mutual inductance M and the ESRs R1 and R2. Since M is a variable that depends on the power transfer distance and it is difficult to precisely determine the values of R1 and R2, practical WPT systems use a tracking process to find $R_{L\eta max}$ instead of predicting it, as shown by the algorithm of the tracking is like the maximum power point tracking (MPPT) algorithm widely used in PV system.

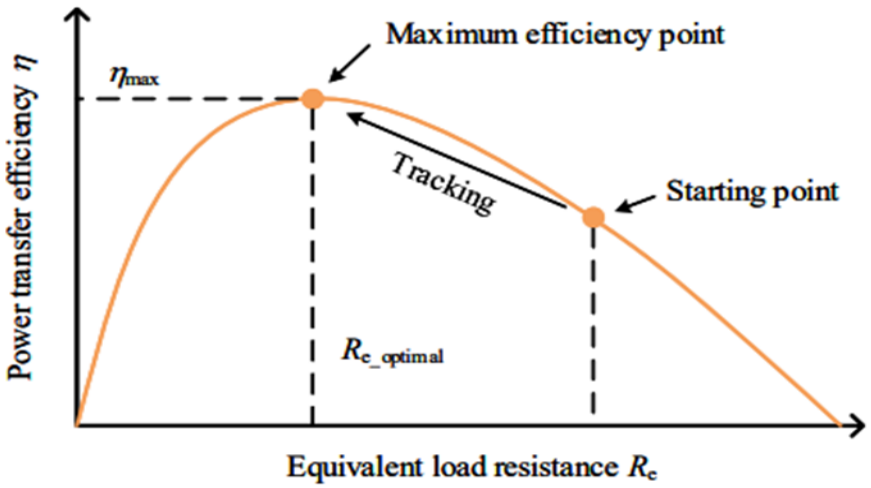

Figure 2-7 Schematic diagram of MEPT

In WPT the objective is to optimize power transfer efficiency, which called MEPT [2-4]. Given that the effective load resistance in a WPT system varies depending on the user, the system must incorporate a control mechanism to adjust Re to its optimal value, enabling MEPT

Table 2-1 the three main differences of the four basic topologies are given of efficiency

Table 2-1: Four fundamental compensation networks

Topologie	SS	SP	PS	PP
System efficiency	$\frac{\omega^2 M^2}{R_p R_L + \omega^2 M^2}$	$\frac{R_L M^2}{R_L M^2 + L_s^2 R_p}$	$\frac{\omega^2 M^2}{R_p R_L + \omega^2 M^2}$	$\frac{R_L M^2}{R_L M^2 + L_s^2 R_p}$

2.3.2 Basic Principles of Maximum Efficiency Point Tracking

The Maximum Efficiency Point (MEPT) analysis in Wireless Power Transfer (WPT) systems assumes that the system primarily experiences Equivalent Series Resistance (ESR) losses. This implies that losses in both the inverter and rectifier are accounted for as ESR losses. Typically, the main power loss in WPT systems occurs from the inverter's input to the rectifier's output. The MEPT control scheme optimizes efficiency by maintaining the operating frequency at the resonant frequency on the

receiving side. It achieves this by adjusting the load resistance using a DC-DC converter to match the optimal value and regulating the input voltage with another DC-DC converter on the transmitting side to control the system's output voltage.

This control scheme relies on two key variables: the input voltage conversion ratio and the load resistance conversion ratio Figure 2.8 shows a schematic plot of a contour line on the mountain

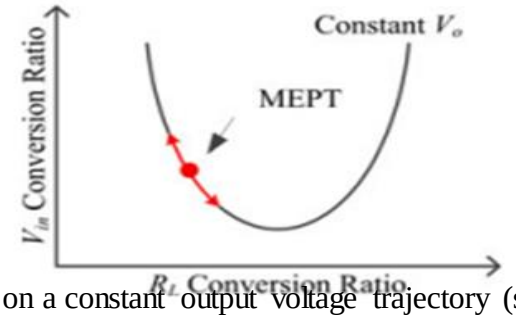

Figure 2-8: MEPT on a constant output voltage trajectory (schematic plot)

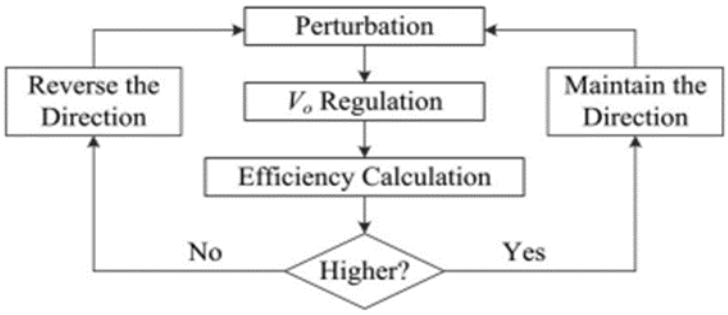

Figure 2-9: Flowchart of the MEPT control scheme

The MEPT control scheme in WPT systems aims to maintain a constant output voltage trajectory while adjusting the system's operating point along this trajectory to achieve maximum efficiency. This involves continuously tracking and optimizing the equivalent load resistance to align with its optimal value. However, predicting the exact maximum efficiency point becomes challenging due to factors like variable mutual inductance based on placement and the fluctuating Equivalent Series Resistances (ESRs) under different operating conditions. As a result, real-time tracking using the MEPT method becomes essential to dynamically identify and pursue the optimal operating point as conditions change show in Figure 2-9 [3]

2.4 Maximizing Efficiency Control Schemes

For optimal high-power transfer, the system should ideally operate at or near resonance. However, the resonant state can be unstable because it depends on the parameters of resonant components, the magnetic coupling coefficient, and the equivalent load resistance. To sustain resonance, control strategies can be divided into two categories

2.4.1 Resonant Control Schemes

1) Efficiency optimization based on frequency control

In a scenario involving one transmitter and one portable receiver, the efficiency of transfer, influenced by factors like distance, relative orientation, and alignment between the resonators, is denoted as. Notably, the magnitude of this parameter is notably low when the transmitter and receiver are far apart. As they move closer, increases, and at a specific point, frequency splitting occurs, impacting system performance.

Hence, an efficient control mechanism based on frequency regulation is essential to stabilize transfer efficiency. Typically, the control frequency range is limited, with the upper limit determined by coil characteristics and the lower limit by efficiency considerations. Within this range, the frequency can be precisely adjusted for optimal efficiency. However, due to the complexity of calculations involved, it is practical to utilize an approximation of mutual inductance for accurate analysis given as below [1]:

$$M \approx \frac{N_2 N_3}{2D^3}\,\pi\mu_0 (r_2 r_3)^2 \qquad (2\text{-}28)$$

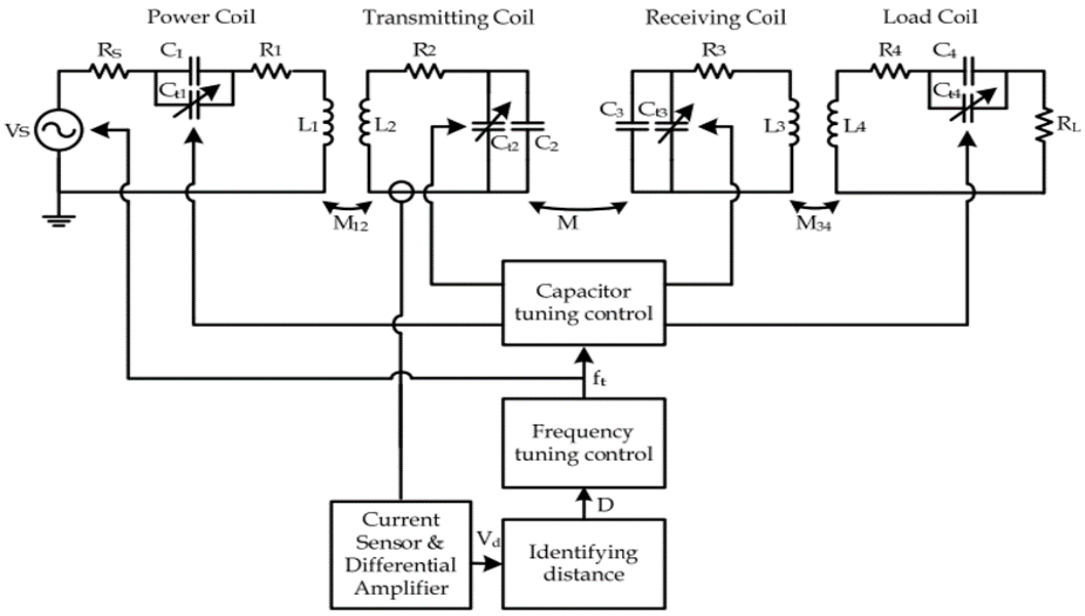

Figure 2-10: Adaptive circuit of frequency control.

A circuit designed to adaptively maintain the system's transfer efficiency is illustrated in Figure 2-9. This circuit employs a current sensor to monitor the current flowing through the transmitting coil. Since the transmitting coil is not grounded, the detected signal is in the form of a differential signal. The signal is then compared to reference sources in a nearby block, necessitating the use of a differential amplifier to convert the differential signal into a single-ended signal. The resulting output

voltage, V_d, is then directed to a distance identification block, where it is compared to reference voltages to determine the distance between the resonators [1]

2) Efficiency optimization based on impedance matching control

The controllable impedance matching method, as a promising option for enhancing transmission efficiency, effectively addresses resonant state mismatches resulting from changes in coupling conditions. This is achieved by employing a controllable resonant unit to broaden the resonant operating range without the need for additional control circuits. Notably, the controllable resonant units primarily consist of a capacitor array and a reconfigurable loop array.

2.4.2 Equivalent Load Resistance Adjustment

1) Equivalent Load Resistance by the DC-DC converter

DC-DC converters are designed to adapt the input voltage to the desired output voltage, which is typically used in the secondary side of wireless power transfer (WPT) systems to regulate both output voltage and power. Additionally, DC-DC converters can be employed to manage the equivalent load resistance to achieve maximum efficiency by transforming the load resistance to its optimal value. Figure 2.11 illustrates a WPT system where a DC-DC converter is connected behind the rectifier, with Uin and U_{out} representing the input and output voltages, respectively. The equivalent resistance (R_e) seen from the output of the rectifier and the load resistance (R_L) are also depicted. The relationship between these resistances can be derived assuming no power loss [1]:

$$\frac{U_{in}^2}{R_e} = \frac{U_{out}^2}{R_L} \tag{2-29}$$

The DC–DC converters can be generally divided into three categories of buck, boost, and buck–boost

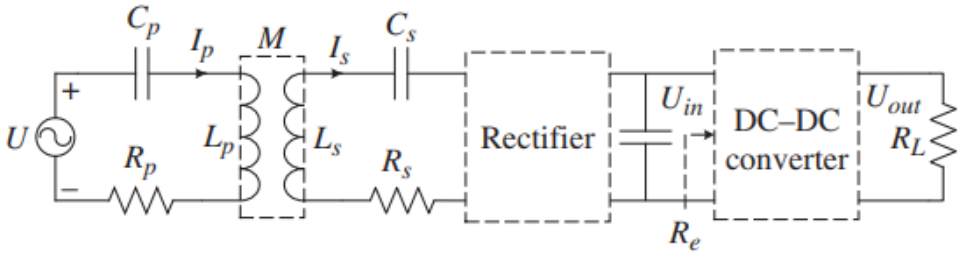

Figure 2-11: Equivalent circuit of a WPT system with the DC-DC converter connecting behind the rectifier.

The transfer characteristics of the basic converters are shown in Table 2.2

Table 2-2 comparison of the basic converters

Topology	Output voltage	Equivalent load resistance	Regulating range	Input current

buck	DU_{in}	$\frac{R_L}{D_2}$	$R_L \sim \infty$	Discontinuous
boost	$\frac{1}{1-D}\ U_{in}$	$(1-D)R_L$	$0 \sim R_L$	Continuous
Buck- boost	$\frac{D}{1-D}\ U_{in}$	$\left(\frac{1-D}{D}\right)R_L$	$0 \sim \infty$	Discontinuous
Cascaded boost- buck	$\frac{D_2}{1-D_1}\ U_{in}$	$\left(\frac{1-D_1}{D_2}\right)R_L$	$0 \sim \infty$	Continuous

By adjusting the duty cycle of the DC-DC converter, the equivalent load resistance can be transformed to the optimal value, even when the coupling state and load resistance are varying. Typically, optimal load resistance closed-loop control schemes can be categorized into two types: secondary-side control and dual-side control, as depicted in the block diagrams shown in Figure 2-12. For the secondary-side control approach, the controllable variable of the voltage conversion ratio r can be expressed as: [1]

$$r = \frac{U_{out}}{U_s} \tag{2-30}$$

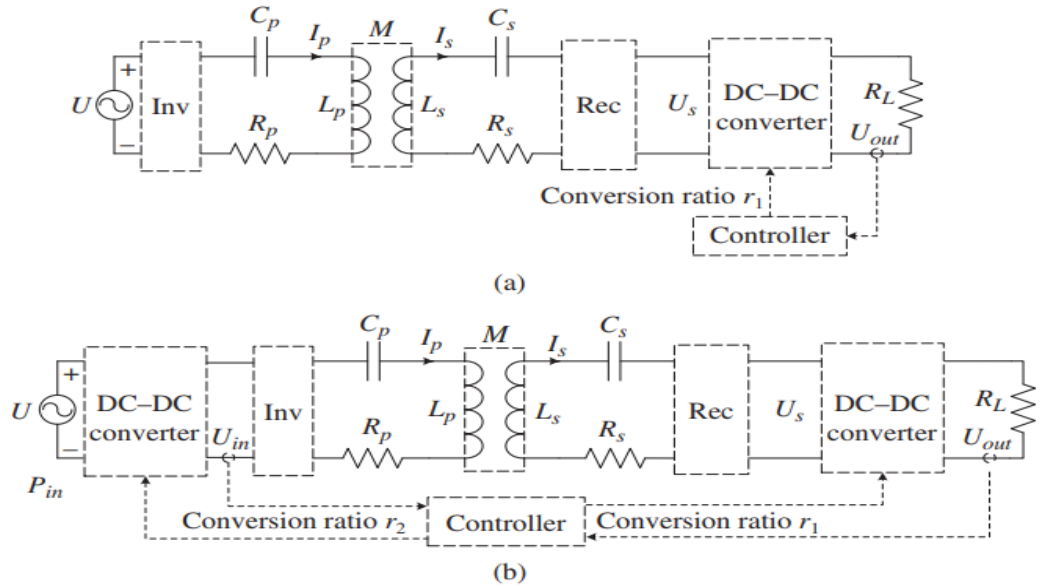

Figure 2-12: Diagram of the optimal load resistance closed-loop control schemes: (a) secondary-side control; (b) dual-side control.

$$\begin{cases} r_1 = \frac{U_p}{U_{dc}} \\ r_2 = \frac{U_{out}}{U_s} \end{cases} \tag{2-31}$$

where U_p, U_{dc}, U_s, and U_{out} are the input and output voltages of the primary and secondary DC–DC converter, respectively. [1]

2) Using Active Rectifier in the Secondary Side:

Several studies have explored using active rectifiers to adjust the equivalent load resistance. A typical WPT system circuit with an active rectifier on the secondary side is shown in Figure 2-13. Replacing some or all of the diodes in a full-bridge rectifier with active switches allows control of the output voltage by adjusting the switches' turn-on time. Common modulation schemes used for this purpose include pulse-width modulation (PWM) and pulse-density modulation (PDM) [1]

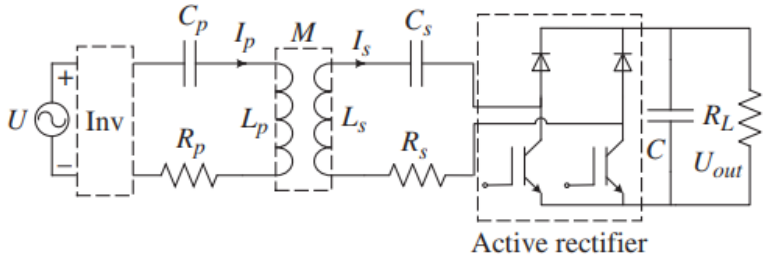

Figure 2-13: Equivalent circuit of a WPT system with the active rectifier in the secondary side

PWM control regulates the output voltage by adjusting the phase-shift angle between the two legs of the rectifier. This allows active rectifiers to operate in a manner similar to passive rectifiers [1]. The Fundamental output voltage can Be calculated using the Fourier series of a boost converter

$$U_{\text{in}} = \frac{2\sqrt{2}}{\pi} U_{\text{out}} \sin\left(\frac{D\pi}{2}\right) \tag{2-32}$$

The pulse width of the secondary voltage (D) and the duty cycle of the active switches (1-D) are calculated by substituting (2-33) into (2-29).

$$\mathrm{R_e} = \frac{4}{\pi^2} \mathrm{R_L}[1 - \cos(D\pi)] \tag{2-33}$$

The pulse density, a measure of the number of pulses divided by the number of switching cycles, is controlled by adjusting the switching times of Q1 and Q2.

$$\mathrm{U_{in}} = \frac{2\sqrt{2}}{\pi} \mathrm{U_{out}} \mathrm{D} \tag{2-34}$$

To compute the equivalent load resistance, substitute (2-34) into (2-29) where D represents the pulse width of the secondary voltage and 1–D represents the duty cycle of active switches [1].

$$\mathrm{R_e} = \frac{8}{\pi^2} \mathrm{R_L}\, \mathrm{D}^2 \tag{2-35}$$

Active rectifiers can manipulate equivalent load resistance by regulating pulse width D, reducing system costs but constricting adjustability compared to DC-DC converters.

2.5 Modeling of Boost Converter

A DC-DC converter is an electronic circuit that converts DC voltage from one value to another using power electronics. It also converts current from a low value to a higher one, meaning that the power remains constant during the conversion process. This is a key distinction of DC-DC converters from voltage reducers and regulators, which consume power during voltage conversion

2.5.1 Mathematical Modeling of Boost Converters

Figure 2-14 depicts the electrical circuit model of the plant, which incorporates parasitic resistances. In the context of continuous conduction mode (CCM) operation, this configuration [17].

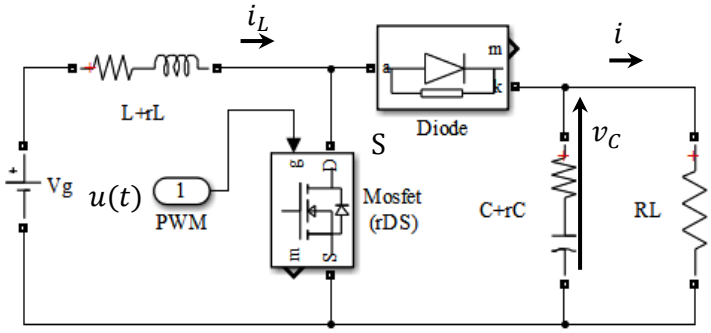

Figure 2-14: Basic Boost Converter.

The system under consideration can be characterized in state-space representation as a switched linear system [17].

$$\begin{cases} \dot{x} = A_i x + B_i v_g \\ v_c = C_i x \end{cases} \quad (2\text{-}36)$$

with two subsystems whose descriptions depend on the state of the switch S. Choosing the state vector as $x^T = [x_L \; x_C]^T$ [17], where the superscript (T) denotes transpose, the model of the subsystem concerning the switch on is given by the matrices $V_0 = C_i X$.

$$A_1 = \begin{bmatrix} -\frac{r_S + r_{DS}}{L} & 0 \\ 0 & -\frac{1}{C(R_L + r_c)} \end{bmatrix} \qquad B_1 = \begin{bmatrix} \frac{1}{L} \\ 0 \end{bmatrix} \qquad C_1 = \begin{bmatrix} 0 & \frac{R_L}{R_L + r_c} \end{bmatrix} \quad (2\text{-}37)$$

The subsystem pertaining to the switch-off state is provided by

$$A_2 = \begin{bmatrix} -\frac{R_L(r_L + r_c) + r_L r_c}{L(R_L + r_c)} & -\frac{R_L}{L(R_L + r_c)} \\ -\frac{R_L}{C(R_L + r_c)} & -\frac{1}{C(R_L + r_c)} \end{bmatrix} \quad B_1 = \begin{bmatrix} \frac{1}{L} \\ 0 \end{bmatrix} \qquad C_1 = \begin{bmatrix} \frac{R_L r_c}{R_L + r_c} & \frac{R_L}{R_L + r_c} \end{bmatrix} \quad (2\text{-}38)$$

From equations (2-37) - (2-38) the average model can be derived.

$$\begin{cases} \dot{\bar{x}} = A\bar{x} + B v_g \\ \overline{v_0} = C\bar{X} \end{cases} \quad (2\text{-}39)$$

whose matrices are given by

$$\begin{aligned} A &= A_1 D + A_2 D' \\ B &= B_1 D + B_2 D' \\ C &= C_1 D + C_2 D' \end{aligned} \quad (2\text{-}40)$$

where D is the nominal duty cycle and $D' = 1 - D$. The equilibrium point is determined through [17]

$$X_q = -A^{-1}Bv_g \tag{2-41}$$

Given that the converter operates around a specific equilibrium point and experiences minor perturbations, a linearized state-space model of the plant can be formulated as follows

$$\begin{cases} \dot{\hat{x}} = F\hat{x} + G\hat{d} \\ \hat{v}_0 = H\hat{x} + E\hat{d} \end{cases} \tag{2-42}$$

where $\hat{d}$ represents a small perturbation introduced in the control signal, and the system matrices are expressed as

$$\begin{gathered} \mathrm{F} = \mathrm{A} \\ \mathrm{G} = (A_1 + A_2)X_q \\ \mathrm{H} = \mathrm{C} \\ \mathrm{E} = (C_1 + C_2)X_q \end{gathered} \tag{2-43}$$

2.6 Control Strategies for Boost Converters in WPT

2.6.1 Perturbation and Observation (P&O)

The P&O method is commonly used to achieve Maximum Power Transfer (MPPT) for photovoltaic converters, similar to MEPT for WPT systems. MEPT is achieved by adding a series of perturbations with illustrates the flowchart of the P&O-based MEPT method, with the secondary DC-DC converter adjusting the conversion ratio r1 and the primary DC-DC converter regulating the output power by adjusting the conversion ratio $r2$. The corresponding block diagram is shown in Figure 2-16 [1].

1. Define the expected system efficiency ηe and initialize the conversion ratios r_1 and r_2
2. Apply a small and constant perturbation $\Delta r1$ incrementally to adjust the equivalent load resistance, ensuring control accuracy and stability.
3. Measure the output power $Pout$ and regulate it to the desired value by adjusting the conversion ratio r_2.
4. After each perturbation, calculate and record the real-time system efficiency η_t following the regulation of the output power.
5. If $\eta_t > \eta_{t-1}$, it indicates that the adjusted equivalent load resistance is approaching the optimal value, and a perturbation with the same sign should be applied in the next stage. Conversely,
6. if $\eta_t < \eta_{t-1}$, it indicates that the adjusted equivalent load resistance is deviating from the optimal value, and a perturbation with the opposite sign should be applied. These steps are

repeated until the system efficiency matches the expected value η_e, at which point the control procedure is completed.

This method eliminates the need for wireless communication between the primary and secondary sides, thereby enhancing control stability and response speed. [1]

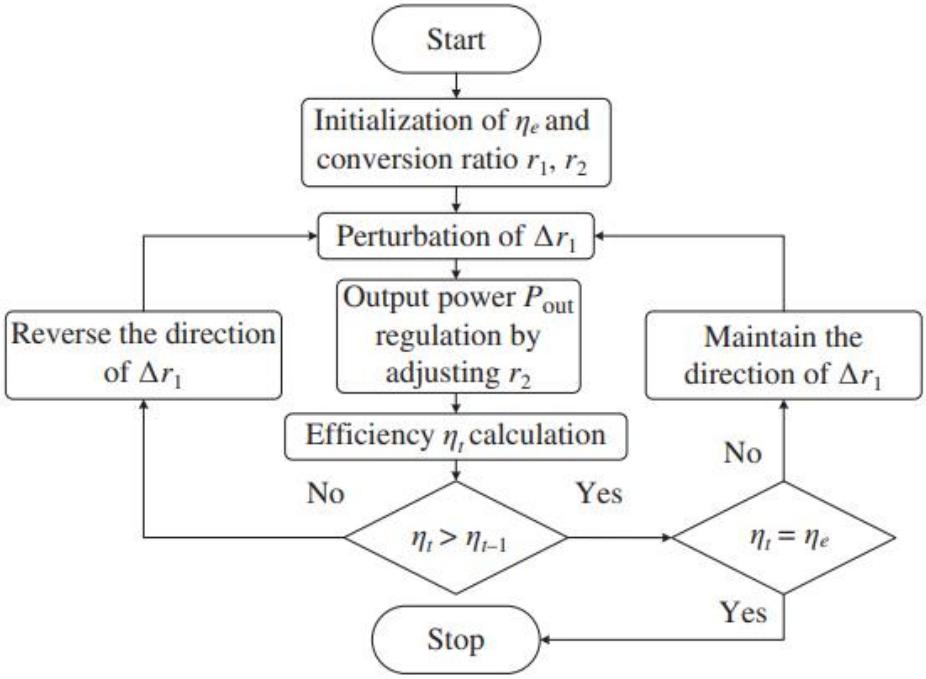

Figure 2-15: Flowchart of P&O-based maximum efficiency point tracking scheme with wireless communication link.

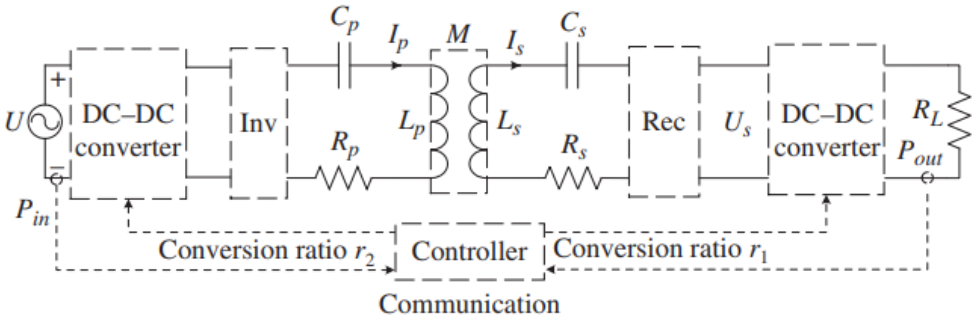

Figure 2-16: Diagram of P&O-based maximum efficiency point tracking control schemes: with wireless communication link

2.7 Conclusion

In this chapter, we introduced the static DC-DC boost converter used in this work. Then, we explained the principle of maximum power point finding and the evaluation criteria of MEPT controls. We introduced the methods based on power feedback, such as the inductance increment method, the perturbation and observation method.

Chaptre 3: Simulation Results and Discussion

3.1 Introduction

In this chapter, a series of simulation tests are conducted to evaluate the performance of the proposed WPT system. The results are systematically presented and analyzed to assess key performance indicators, such as system efficiency and output voltage. These metrics are examined across varying conditions, including changes in system parameters, to provide a comprehensive understanding of the WPT system's capabilities under different operational scenarios.

3.2 Verification of Steady-State Model

Table 3-1:parameters of the WPT System

Parameter	Explanation	Value
L1	Inductance of the sending resonator	34 µH
L2	Inductance of the receiving resonator	34 µH
M	Mutual inductance between L1 and L2	7.33 µH
C1	C1 Capacitance of the sending resonator	117 nF
C2	Capacitance of the receiving resonator	117 nF
Cf	Capacitance of the output filter	300 µF
R1	Equivalent resistance of the L1, C1 branch	0.039 Ω
R2	Equivalent resistance of the L2, C2 branch	0.039 Ω
Rs	On-state resistance of the switches	0.001 Ω
RL	Load resistance	5 Ω
Vr	Forward voltage of the diodes	0.8 V
Vd	Voltage of the DC source	400 V
fs	Switching frequency of the inverter	80 Hz

3.2.1 System efficiency

Using the parameters listed in Table 3-1, the system efficiency is calculated and plotted as a function of the coupling coefficient and load resistance in Figure 3-1.The system efficiency for switching frequency and load is calculated and plotted in Figure 3-2 shows that the efficiency decreases as the coupling weakens. For a constant coupling coefficient, there is a corresponding load resistance that achieves maximum efficiency.

Figure 3- 2shows that as the switching frequency increases or decreases above a certain threshold, the efficiency becomes 0

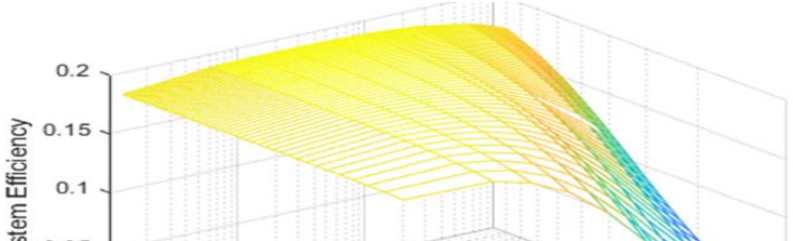

Figure 3-1: Efficiency as function of coupling coefficient and load resistance

.

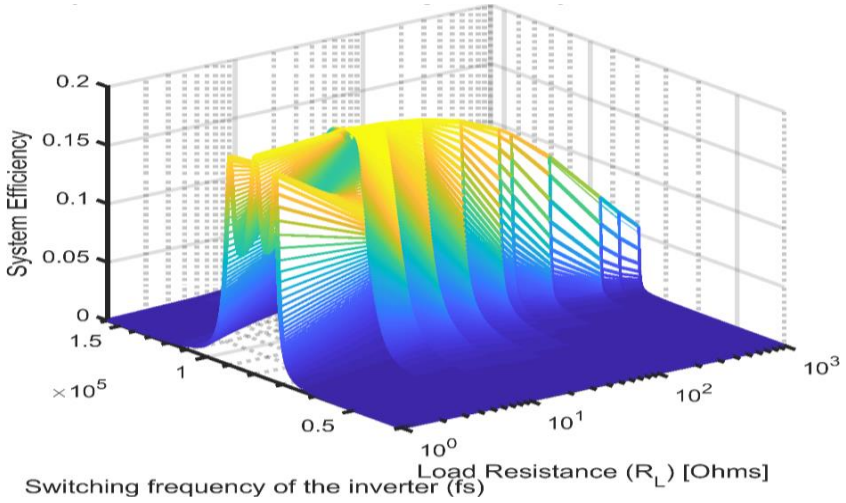

Figure 3-2: Efficiency as function of switching frequency of the inverter and load resistance

3.3 Simulation of the Proposed WPT

3.3.1 Open Loop System

In The simulation a resistive load, that simulates a battery (R_L), is considered. At this point, the WPT can be set up as illustrated in the Figure 3-3 Circuit simulation to extract voltage and current results, primary, secondary and output waveforms of voltage and current output from the inverter under 0.8pi reference and use reference Table 3-1.

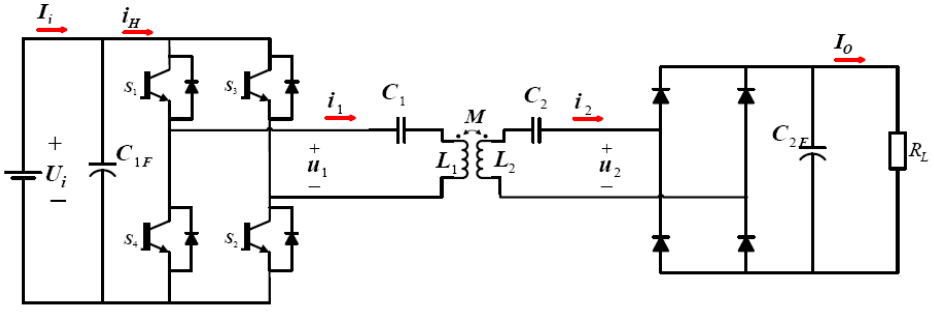

Figure 3-3: Electrical circuit of compensated IPT system with a resistive load

Simulation results

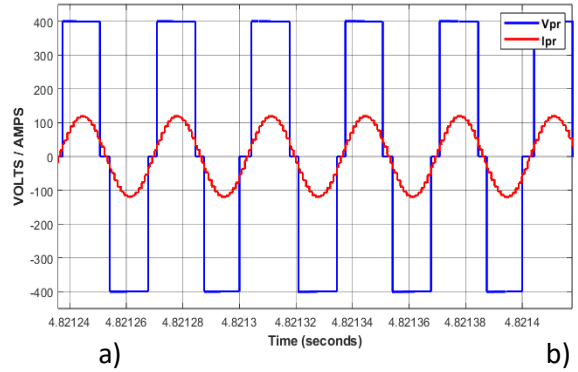

a)

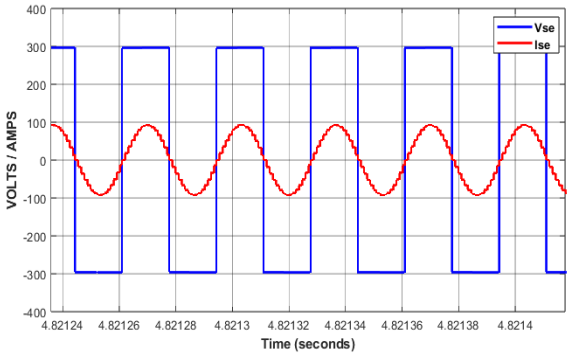

b)

Figure 3-4 : Voltage and current a) primary-side b) secondary-side

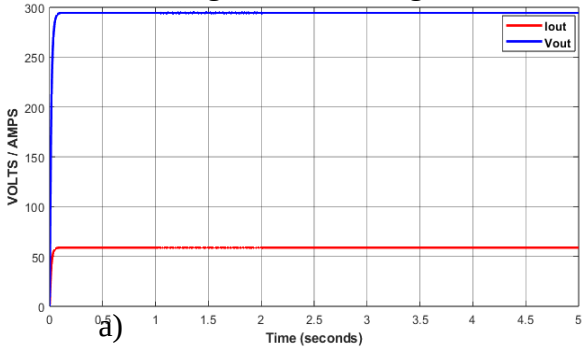

a)

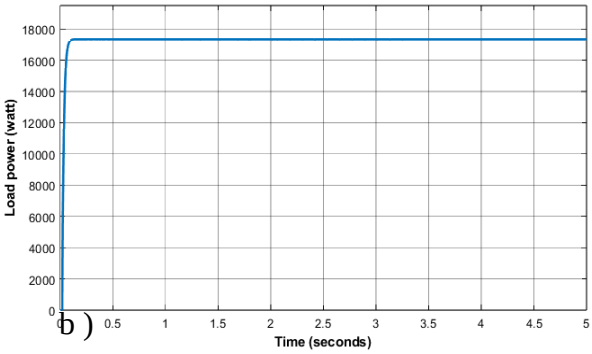

b)

Figure 3-5 : a) load voltage and current. b) load power

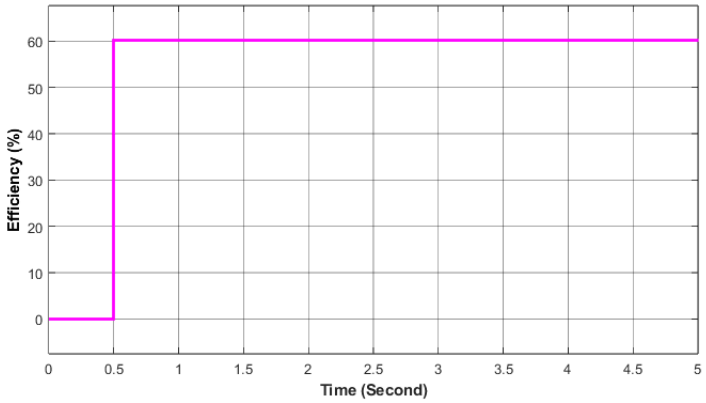

Figure 3-6: efficiency

3.3.2 Closed Loop System

Figure 3.7 illustrates a schematic diagram of the WPT system used in the simulation study. Three resistor values are incorporated into the simulation: 10Ω, 15Ω, and 30Ω. The resistance values change over time as follows:

- From 0 to 5 seconds: RL = 10Ω
- From 5 to 10 seconds: RL = 15Ω

- From 10 to 15 seconds: RL = 30Ω

The simulation is conducted under two scenarios: with the MEPT-based P&O algorithm and without it. Identical parameters are maintained in both cases to facilitate a direct comparison and to assess the effectiveness of the proposed algorithm.

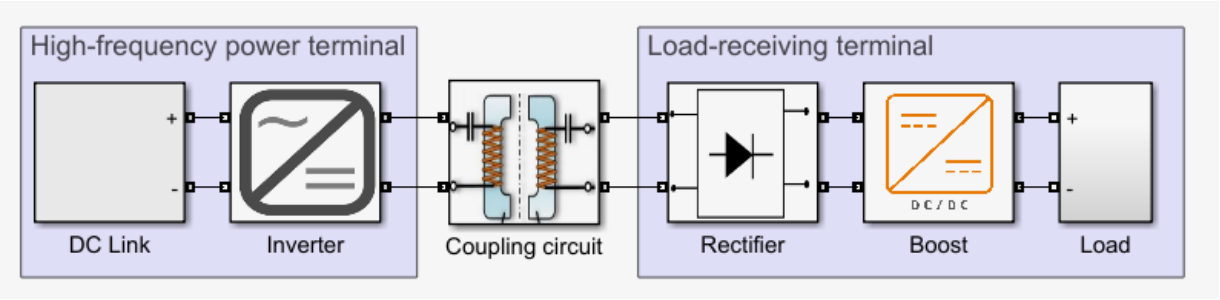

Figure 3-7: Block diagram of WPT used in simulation

Figure 3.8 shows the simulation model of a boost converter within a WPT system. The converter regulates voltage to ensure efficient power transfer, adjusting the load dynamically with a Maximum Efficiency Point Tracking (MEPT) algorithm. This helps optimize power transfer under varying load conditions.

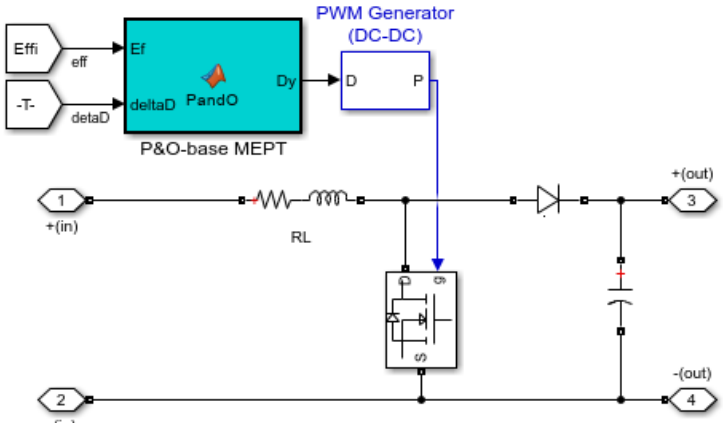

Figure 3-8: Simulation model of a boost converter with a P&O algorithm.

1) **Simulation Results**

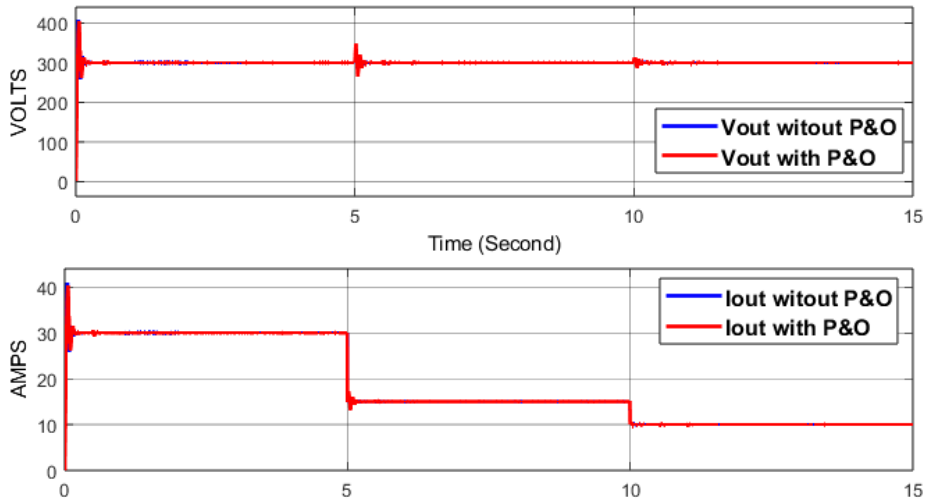

Figure 3-9 : load voltage and current

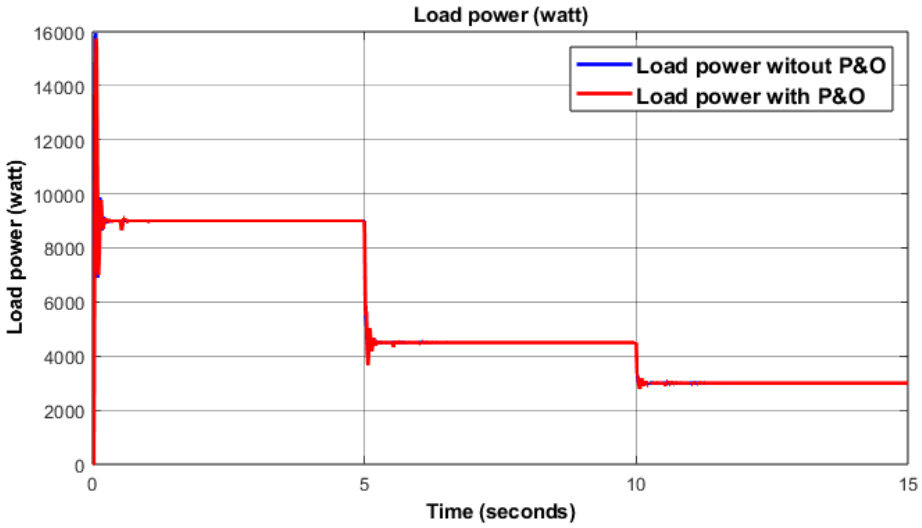

Figure 3-10 :load power

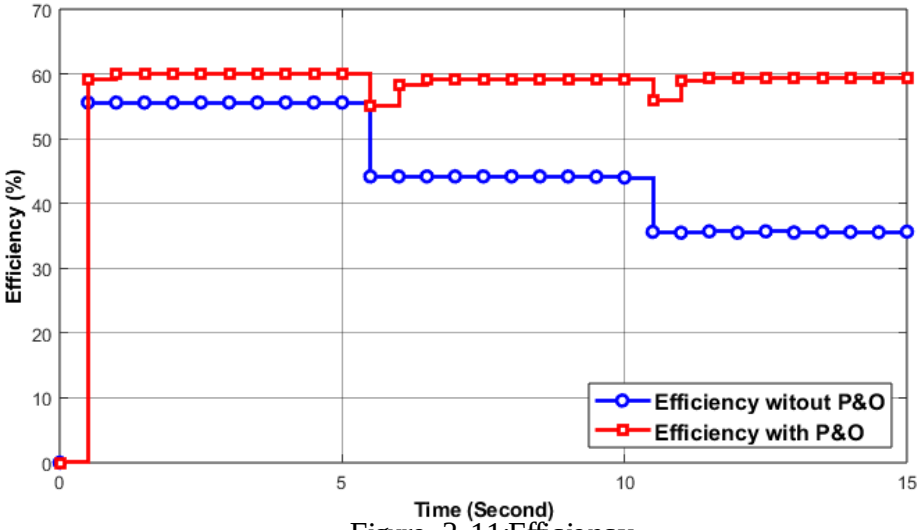

Figure 3-11:Efficiency

2) Efficiency Analysis

Efficiency is a key performance indicator in WPT systems, and Figure 3.11 shows a clear advantage for the system utilizing the MEPT algorithm. The efficiency remains high and relatively stable across the different resistance values, demonstrating the algorithm's ability to maintain optimal power transfer. The algorithm adjusts the system to match the load demands, preventing energy wastage.

Without the MEPT algorithm, the efficiency drops significantly, especially when the load resistance increases. This highlights the inefficiency of the system in transferring power without dynamic adjustment, leading to wasted energy and lower overall system performance.

In summary, the results clearly demonstrate that the inclusion of the MEPT-based P&O algorithm significantly improves the performance of the WPT system across all metrics. The system with the algorithm maintains higher and more stable load power, voltage, and efficiency compared to the non-

MEPT scenario, particularly under varying load conditions. This reinforces the importance of dynamic load adjustment algorithms in optimizing WPT system performance.

3.4 Conclusion

This chapter presented a detailed evaluation of the proposed Wireless Power Transfer (WPT) system through a series of simulations. The results emphasized key metrics, such as system efficiency, load voltage, current, and power transfer, under varying load conditions. The inclusion of the Maximum Efficiency Point Tracking (MEPT)-based Perturb and Observe (P&O) algorithm significantly improved performance.

The MEPT algorithm enabled the system to maintain higher efficiency, stable voltage, and optimal power transfer despite changes in load resistance. In contrast, the system without MEPT experienced reduced efficiency and unstable performance, particularly with higher resistance values.

Overall, the simulations demonstrate the clear advantages of incorporating dynamic load adjustment algorithms, such as MEPT, in WPT systems. These algorithms enhance power transfer efficiency, reduce energy losses, and ensure stable operation under various conditions, making them essential for reliable wireless power transmission applications.

General conclusion

This research focused on the design and control of dynamic wireless power transfer (WPT) systems, particularly for electric vehicle charging. By employing a boost converter and the Perturbation and Observation (P&O) algorithm, the study demonstrated improvements in power transfer efficiency. The simulations confirmed that dynamic WPT can effectively support wireless vehicle charging while maintaining high efficiency.

Key Findings The integration of a boost converter with the P&O algorithm optimized power transfer, adapting to varying load conditions. This resulted in a stable and efficient wireless charging system, addressing the growing need for flexible and reliable electric vehicle charging solutions.

Contributions This study advances control methods for dynamic WPT applications, particularly in electric vehicle charging, providing a practical framework that bridges theory and real-world application. The use of an efficient MPPT-based control strategy offers valuable insights for future wireless power transfer systems.

Future Directions

- **Algorithm Development**: Future research could explore machine learning-based MPPT methods to further enhance system adaptability.
- **Practical Testing**: Implementing real-world tests would offer more robust insights into system performance under varying conditions.
- **Multi-vehicle Optimization**: Research could focus on enabling simultaneous charging of multiple vehicles.
- **Safety Measures**: Further studies are necessary to address safety concerns and minimize electromagnetic interference (EMI).

This work lays the groundwork for future advancements in dynamic WPT, with significant potential for impact in the electric vehicle industry and other wireless charging applications.

.

Bibliography

[1] Z. Zhang and H. Pang, Wireless Power Transfer: Principles and Applications, John Wiley & Sons, 2022.

[2] X. a. Z. C. a. S. H. Zhang, Wireless Power Transfer Technologies for Electric Vehicles, Springer, 2022.

[3] H. Li, J. Li, K. Wang, W. Chen and X. Yang, "A maximum efficiency point tracking control scheme for wireless power transfer systems using magnetic resonant coupling," *IEEE Transactions on Power Electronics,* vol. 30, p. 3998–4008, 2014.

[4] C. A. Baguley, S. G. Jayasinghe and U. K. Madawala, "Theory and control of wireless power transfer systems," in *Control of Power Electronic Converters and Systems*, Elsevier, 2018, p. 291–307.

[5] S. R. Hui, "Past, present and future trends of non-radiative wireless power transfer," *CPSS Transactions on Power Electronics and Applications,* vol. 1, p. 83–91, 2016.

[6] Z. a. P. H. a. G. A. a. C. C. Zhang, "Wireless power transfer - An overview," *IEEE transactions on industrial electronics,* vol. 66, no. 2, pp. 1044--1058, 2018.

[7] T. A. A. H. M. E. D. FARNANA, "ANALYSIS AND COMPARISON OF CLASSICAL COMPENSATION TOPOLOGIES FOR INDUCTIVE POWER TRANSFER FOR ELECTRICAL VEHICLES".

[8] P. Pérez-Nicoli, F. Silveira and M. Ghovanloo, Inductive Links for Wireless Power Transfer, Springer, 2021.

[9] T. Imura and T. Imura, Wireless power transfer, Springer, 2020.

[10] M. Amjad, M. Farooq-i-Azam, Q. Ni, M. Dong and E. A. Ansari, "Wireless charging systems for electric vehicles," *Renewable and Sustainable Energy Reviews,* vol. 167, p.

112730, 2022.

[11] J. M. Miller, C. P. White, O. C. Onar and P. M. Ryan, "Grid side regulation of wireless power charging of plug-in electric vehicles," in *2012 IEEE energy conversion congress and exposition (ECCE)*, 2012.

[12] S. Jeong, Y. J. Jang and D. Kum, "Economic analysis of the dynamic charging electric vehicle," *IEEE Transactions on Power Electronics,* vol. 30, p. 6368–6377, 2015.

[13] Y. J. Jang, E. S. Suh and J. W. Kim, "System architecture and mathematical models of electric transit bus system utilizing wireless power transfer technology," *IEEE Systems Journal,* vol. 10, p. 495–506, 2015.

[14] E. {Coca, {Wireless power transfer: fundamentals and technologies}, {. o. Demand}, Ed., {2016}.

[15] F. Chen, H. Garnier, Q. Deng, M. K. Kazimierczuk and X. Zhuan, "Control-oriented modeling of wireless power transfer systems with phase-shift control," *IEEE Transactions on Power Electronics,* vol. 35, p. 2119–2134, 2019.

[16] H. Li, J. Fang, S. Chen, K. Wang and Y. Tang, "Pulse density modulation for maximum efficiency point tracking of wireless power transfer systems," *IEEE Transactions on Power Electronics,* vol. 33, p. 5492–5501, 2017.

[17] A. Emadi, "Modeling and analysis of multiconverter DC power electronic systems using the generalized state-space averaging method," *IEEE Transactions on Industrial Electronics,* vol. 51, p. 661–668, 2004.

[18] W. Zhong, D. Xu and R. Y. Hui, "Wireless Power Transfer," in *Between Distance and Efficiency, Zhejiang University*, Springer, 2020.

[19] S. Wang, B. Wei, C. Gao, C. Xu, X. Wu, C. Cui, F. Zhou and Y. Liu, "Modeling and control methods of dynamic wireless power transfer system," in *2017 IEEE Transportation Electrification Conference and Expo, Asia-Pacific (ITEC Asia-Pacific)*, 2017.

[20] C. T. Rim and C. Mi, Wireless power transfer for electric vehicles and mobile devices, John Wiley & Sons, 2017.

[21] Y. Lu and D. B. Ma, "Wireless power transfer system architectures for portable or implantable applications," *Energies,* vol. 9, p. 1087, 2016.

[22] K. Hata, T. Imura and Y. Hori, "Dynamic wireless power transfer system for electric vehicles to simplify ground facilities-power control and efficiency maximization on the secondary side," in *2016 IEEE applied power electronics conference and exposition (APEC)*, 2016.

[24] J. I. Agbinya, Wireless power transfer, River Publishers, 2022.

[25] X. Zhang, C. Zhu and H. Song, Wireless Power Transfer Technologies for Electric Vehicles, Springer, 2022.

الجمهورية الجزائرية الديمقراطية الشعبية

République Algérienne Démocratique et Populaire

وزارة التعليم العالي والبحث العلمي

Ministère de l'Enseignement Supérieur Et de La Recherche Scientifique

جامعة غرداية

Faculté des sciences et Technologies

Département d'automatique et d'électromécanique

كلية العلوم والتكنولوجيا

قسم الآلية والكهروميكانيك

Université de Ghardaïa

غرداية في: ....

إذن بالطباعة (مذكرة ماستر)

بعد الاطلاع على التصحيحات المطلوبة على محتوى المذكرة المنجزة من طرف الطلبة التالية أسماؤهم:

1. الطالب (ة): بطاش طارق
2. الطالب (ة): رحيم كوثر

تخصص: ماستر الية و انظمة

نمنح نحن الأستاذ (ة):

الاسم واللقب	الرتبة – الجامعة الأصلية	الصفة	الامضاء
بخاري عامر	استاذ محاضر ب - جامعة غرداية	رئيسا	
محسن شكوان	أستاذ - جامعة غرداية	ممتحن [illegible]	
[illegible]	استاذ محاضر ب - جامعة غرداية	ممتحن	
[illegible]	أستاذ محاضر أ - جامعة غرداية	مؤطر	

الإذن بطباعة النسخة النهائية لمذكرة ماستر الموسومة بعنوان

Modeling and controle methods of dynamic wireless power transfer (WPT) system

إمضاء رئيس القسم

العلمي عبد اللطيف

رئيس قسم الآلية

و الكهروميكانيك

جامعة غرداية

قسم الآلية والكهروميكانيك -1-

كلية العلوم و التكنولوجيا